

Soil Moisture Influence on Seasonality and Large-Scale Circulation in Simulations of the West African Monsoon

ALEXIS BERG^a

International Research Institute for Climate and Society, Earth Institute, Columbia University, Palisades, New York

BENJAMIN LINTNER

Department of Environmental Sciences, Rutgers, The State University of New Jersey, New Brunswick, New Jersey

KIRSTEN FINDELL

NOAA/Geophysical Fluid Dynamics Laboratory, Princeton, New Jersey

ALESSANDRA GIANNINI

International Research Institute for Climate and Society, Earth Institute, Columbia University, Palisades, New York

(Manuscript received 10 December 2015, in final form 8 November 2016)

ABSTRACT

Prior studies have highlighted West Africa as a regional hotspot of land–atmosphere coupling. This study focuses on the large-scale influence of soil moisture variability on the mean circulation and precipitation in the West African monsoon. A suite of six models from the Global Land–Atmosphere Coupling Experiment (GLACE)-CMIP5 is analyzed. In this experiment, model integrations were performed with soil moisture prescribed to a specified climatological seasonal cycle throughout the simulation, which severs the two-way coupling between soil moisture and the atmosphere. Comparison with the control (interactive soil moisture) simulations indicates that mean June–September monsoon precipitation is enhanced when soil moisture is prescribed. However, contrasting behavior is evident over the seasonal cycle of the monsoon, with core monsoon precipitation enhanced with prescribed soil moisture but early-season precipitation reduced, at least in some models. These impacts stem from the enhancement of evapotranspiration at the dry poleward edge of the monsoon throughout the monsoon season, when soil moisture interactivity is suppressed. The early-season decrease in rainfall with prescribed soil moisture is associated with a delayed poleward advancement of the monsoon, which reflects the relative cooling of the continent from enhanced evapotranspiration, and thus a reduced land–ocean thermal contrast, prior to monsoon onset. On the other hand, during the core/late monsoon season, surface evaporative cooling modifies meridional temperature gradients and, through these gradients, alters the large-scale circulation: the midlevel African easterly jet is displaced poleward while the low-level westerlies are enhanced; this enhances precipitation. These results highlight the remote impacts of soil moisture variability on atmospheric circulation and precipitation in West Africa.

1. Introduction

The two-way interactions between soil moisture and the overlying atmosphere represent important controls on near-surface climate over land. Driven by variability in precipitation and atmospheric evaporative demand,

soil moisture variations in turn modulate fluxes of water and heat at the surface. Through this control on water and energy fluxes, soil moisture variations can feed back onto near-surface surface climate (e.g., temperature and humidity); these impacts can extend to the boundary layer vertical structure and thermodynamics and lead to feedbacks on precipitation. Numerous studies have demonstrated such impacts, in both models and observations [see [Seneviratne et al. \(2010\)](#) for an extensive review]. In addition, to the extent that the atmospheric circulation is sensitive to surface conditions, and that the

^a Current affiliation: Department of Civil and Environmental Engineering, Princeton University, Princeton, New Jersey.

Corresponding author e-mail: Alexis Berg, ab5@princeton.edu

local surface feedback response exhibits sufficient amplitude and spatial coherence, soil moisture variations may further force remote impacts through large-scale circulation (Haarsma et al. 2009; Koster et al. 2014).

Soil moisture–atmosphere interactions may be particularly critical in monsoon regions, as monsoon circulations result from a complex interplay of thermodynamic and dynamic processes in the ocean–land–atmosphere system. The West African monsoon (WAM), in particular, has been shown to be sensitive to land–atmosphere interactions over a range of temporal and spatial scales (e.g., Xue et al. 2012). While numerous studies have demonstrated that sea surface temperature (SST) variability is the primary driver (or pacer) of interannual and decadal variability in WAM precipitation (Folland et al. 1986; Giannini et al. 2003; Bader and Latif 2003; Held et al. 2005; Lu and Delworth 2005; Hoerling et al. 2006), soil moisture dynamics (e.g., Zeng et al. 1999; Giannini et al. 2003) and land surface variability more generally (e.g., vegetation; see Xue 1997; Wang et al. 2004; Kucharski et al. 2013) are thought to maintain and amplify WAM variability at these time scales. On intraseasonal time scales, the landmark multimodel Global Land–Atmosphere Coupling Experiment (GLACE; Koster et al. 2004) highlighted West Africa as a hotspot of land–atmosphere coupling in climate models, with the region exhibiting strong sensitivity of precipitation variability to soil moisture variability during the rainy season. Further studies have identified soil moisture variability as a key contributor to particular modes of intraseasonal variability during the monsoon (Taylor 2008; Lavender et al. 2010). Moreover, at the mesoscale, soil moisture gradients have been shown to influence the initiation of convective precipitation during the day (Taylor and Ellis 2006; Taylor et al. 2011).

In the present study, we adopt a slightly different focus and seek to isolate how interactions between soil moisture and the atmosphere may contribute to shaping the mean precipitation and seasonality of the WAM. We explore the following question: To what extent do soil moisture variability and associated feedbacks onto the atmosphere influence large-scale and seasonal aspects of the WAM? Given the uncertainties surrounding current-generation climate model simulations of the WAM (Xue et al. 2010; Roehrig et al. 2013) as well as future projections of the WAM under global warming (e.g., Biasutti 2013; Giannini et al. 2013; Park et al. 2015), mechanistic understanding of the determinants of WAM precipitation is crucial for improving model skill. Understanding the controls on WAM seasonality is also essential; one robust feature of climate model future projections, in global monsoon regions in general but in West Africa in particular, consists of a shift in the seasonal cycle of the

monsoon, with precipitation decreasing at the beginning of the season and increasing toward its end (Biasutti and Sobel 2009; Seth et al. 2013; Biasutti 2013). The processes underlying this response remain unclear, but interpreting these projections arguably requires understanding of the mechanisms influencing WAM seasonality. For both of these aspects, the documented importance of soil moisture–atmosphere processes in the WAM (e.g., Xue et al. 2012) suggests they may play an important role.

To investigate the soil moisture influence on seasonality and large-scale circulation in the WAM, we make use of climate model simulations from the recent GLACE-CMIP5 multimodel experiment (Seneviratne et al. 2013). GLACE-CMIP5 was designed to investigate the role of soil moisture variability, as well as long-term mean soil moisture changes, in the climate system. Thus, several modeling groups performed transient climate change simulations with soil moisture prescribed to a specified climatology. This protocol aims to disable feedbacks to the atmosphere associated with soil moisture variability. It thus affords the opportunity to investigate the role of these processes on seasonality and large-scale circulation in the WAM. Section 2 describes these simulations and the analysis used; section 3 presents simulation results and the analysis of the underlying processes; the principal results and implications of our study are discussed in section 4.

2. Methods

In the context of the GLACE-CMIP5 experiment (Seneviratne et al. 2013), six modeling centers performed transient climate change simulations (SM_FIX) in which total soil moisture was overridden, in each of the models, by the climatological seasonal values for the period 1971–2000 extracted from the historical fully coupled CMIP5 simulation of the same model. The SM_FIX simulations extend over 1950–2100, with transient SSTs, sea ice, and radiative forcing constituent concentrations prescribed from the corresponding CMIP5 simulations, using the historical simulations over 1950–2005 and the representative concentration pathway 8.5 (RCP8.5) scenario thereafter. For each model, SM_FIX thus mirrors the CMIP5 coupled simulation, except that soil moisture is overridden by the simulated present-day climatology, thus severing the two-way interaction of soil moisture with the atmosphere. In each model, soil moisture was prescribed at every level in the soil column. Depending on the model, the present-day climatology used to prescribe soil moisture was calculated at every model time step, daily, or monthly; in the latter case, interpolation between

the midpoints of the adjacent months was used to prescribe data at every simulation time step in the corresponding model. For each model, either the fully coupled CMIP5 simulation or, for some models, a new reference simulation identical to SM_FIX (i.e., with identical oceanic boundary conditions and atmospheric composition) but with interactive soil moisture, was considered as a reference simulation (SM_INT). Thus, for each model, SM_INT includes identical oceanic boundary conditions and atmospheric composition as SM_FIX, but with interactive soil moisture. Note that in some of the previous publications analyzing GLACE-CMIP5 simulations (Seneviratne et al. 2013; Berg et al. 2014, 2015; May et al. 2015), SM_INT was referred to as REF or CTL and SM_FIX as 1A or expA. The models analyzed here are the Geophysical Fluid Dynamic Laboratory (GFDL) Earth System Model with the Modular Ocean Model (GFDL-ESM2M, hereinafter ESM2M); the National Center for Atmospheric Research (NCAR) Community Climate System Model, version 4 (CCSM4); the European Consortium Earth System Model (EC-EARTH) based on the European Centre for Medium-Range Weather Forecasts (ECMWF) modeling systems and developed by a consortium of European research institutions (see www.to.isac.cnr.it/ecearth/); the Max Planck Institute (MPI) for Meteorology Earth System Model (MPI-ESM); and the Institute Pierre-Simon Laplace Coupled Model, version 5A (IPSL-CM5A). Compared to earlier publications based on GLACE-CMIP5 simulations (Seneviratne et al. 2013; Berg et al. 2015; May et al. 2015), our analysis includes a sixth model, the Australian Community Climate and Earth-System Simulator (ACCESS) model, as does the recent study of Lorenz et al. (2016). Note that in contrast to other participating models, ACCESS uses observed SSTs over 1950–2000 in both the SM_INT and SM_FIX experiments (instead of simulated SSTs from the coupled, historical CMIP5 simulation); however, this difference does not affect our conclusions since we compare SM_FIX and SM_INT separately for each model; the comparison for ACCESS is meaningful since both runs have identical SSTs.

Here we compare SM_INT and SM_FIX over 1971–2000. Focusing on this period ensures that both simulations have identical soil moisture climatologies. The comparison thus isolates the effect on climate of soil moisture variability and associated soil moisture–atmosphere interactions. We again stress that our approach is process oriented: we use these targeted, idealized model experiments to probe the role of soil moisture variability and advance our understanding of monsoon land–atmosphere processes. Our goal here is not to evaluate which simulation is more realistic. In any

event, since soil moisture is interactive in the real world, simulation SM_INT should be considered as the more realistic model configuration.

Figure 1 illustrates the difference in soil moisture variability between SM_FIX and SM_INT over 1971–2000 for the ESM2M model. Because only the mean seasonal cycle is retained in SM_FIX, soil moisture daily variability is much larger in SM_INT, in particular toward the more arid Sahelian part of the domain where precipitation is more variable (relative to the mean). Comparing both simulations over a single point illustrates that this is because of differences at both interannual and intraseasonal time scales (we focus on a single pixel in Fig. 1 to avoid smoothing out differences by taking the domain spatial average). Figure 1 is representative of the typical behavior across the model ensemble. For models in which a monthly climatology of soil moisture is prescribed with month-to-month interpolation (ESM2M, MPI-ESM, and CCSM4), the prescribed soil moisture climatology displays no daily variability (Fig. 1), while for models that use either a daily climatology of soil moisture (IPSL-CM5A and EC-EARTH) or a climatology calculated at every model time-step (ACCESS), some residual daily variability remains in the prescribed climatological soil moisture. However, such differences in protocol appear to have little impact on our results (see also section 4c).

3. Results

a. Precipitation response

Figure 2 compares the main rainy season precipitation over West Africa, June–September (JJAS), in simulations SM_INT and SM_FIX. We first point out that, as is common in climate model simulations of the WAM, there is model-to-model variability in the representation of the monsoon and its associated precipitation field (Xue et al. 2010; Roehrig et al. 2013). For reference, observations of monsoon rainfall are shown in Fig. 3. Broadly, in the control (SM_INT) simulation, some models produce a strong monsoon, with rainfall advancing far to the north into the continent (ESM2M); others simulate a weaker monsoon, with precipitation remaining too close to the Gulf of Guinea coast (IPSL-CM5A and ACCESS). We reiterate that the SST fields imposed in each model's SM_INT and SM_FIX runs are taken from the parent CMIP5 simulations (or observations in ACCESS) and thus differ across the models, as can be inferred from Fig. 2; some of the spread in simulated monsoon characteristics doubtlessly arises from intermodel spread in the distribution of SSTs. Despite visible differences between models in their ability to simulate the WAM, Fig. 2 reveals some common responses across the model suite to the

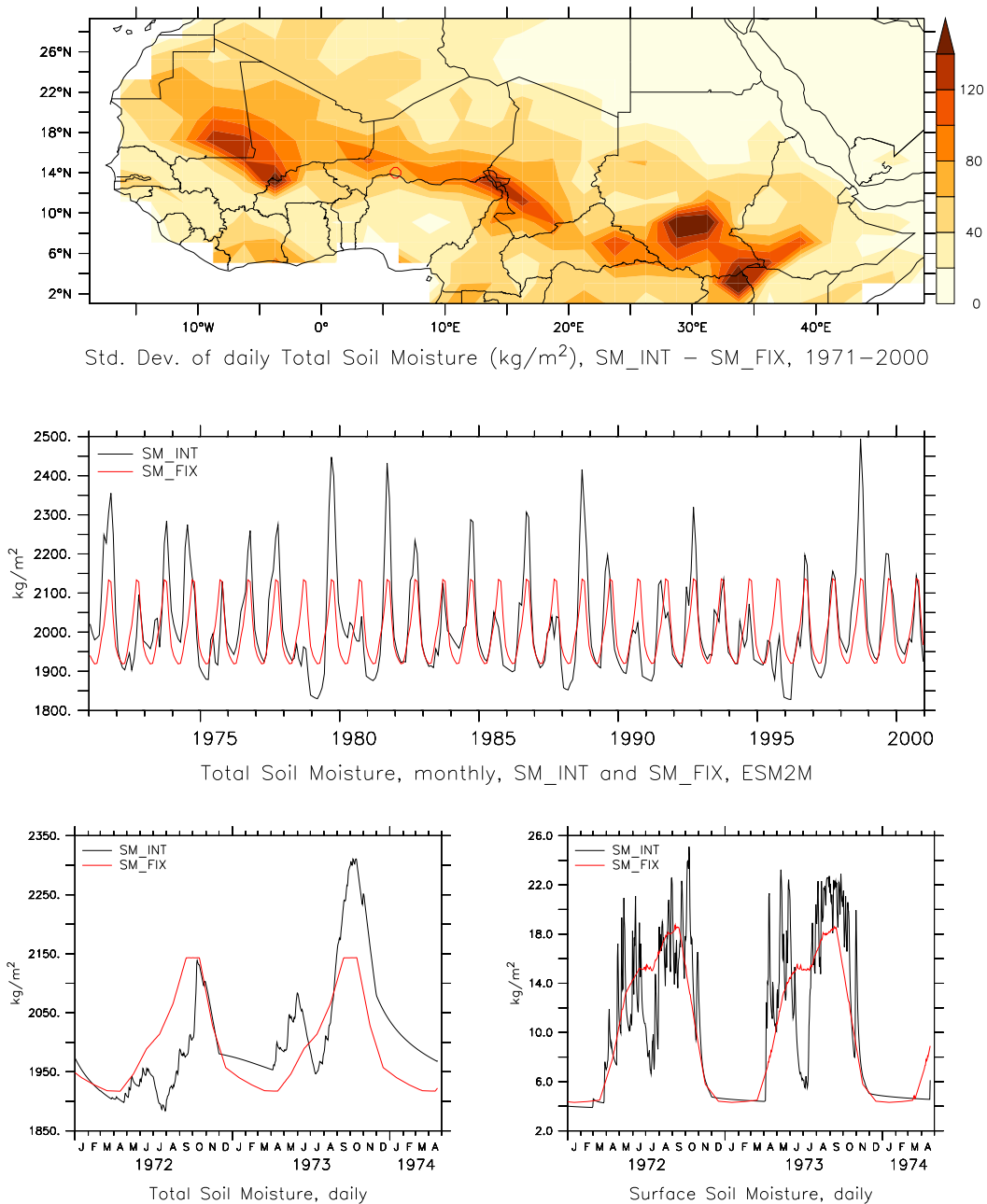


FIG. 1. (top) Difference in standard deviation of daily, total-column soil moisture between SM_FIX and SM_INT over 1971–2000 in ESM2M. (middle) Monthly values over 1971–2000 over one pixel [6°E , 14°N ; see red circle in (top)]. (bottom) Daily values over two seasonal cycles (1972–73) over one pixel (6°E , 14°N) of (left) total-column soil moisture and (right) surface soil moisture (top 10 cm). Note the greater variability in the interactive case of surface soil moisture compared to total soil moisture.

suppression of soil moisture–atmosphere interactions: in all models except MPI-ESM, JJAS precipitation is enhanced in simulation SM_FIX. This response is clearest in ACCESS, ESM2M, EC-EARTH, and IPSL-CM5A. Because of differences in the geographical extent of the simulated monsoon in the models, the location of this

area of enhanced precipitation varies between models; however, Fig. 2 indicates that it tends to lie within (ACCESS and ESM2M) or slightly northward of (EC-EARTH and IPSL-CM5A) the 5 mm day^{-1} isohyet in the different models. In CCSM4, the behavior is more spatially complex, with a zonal band of weak positive

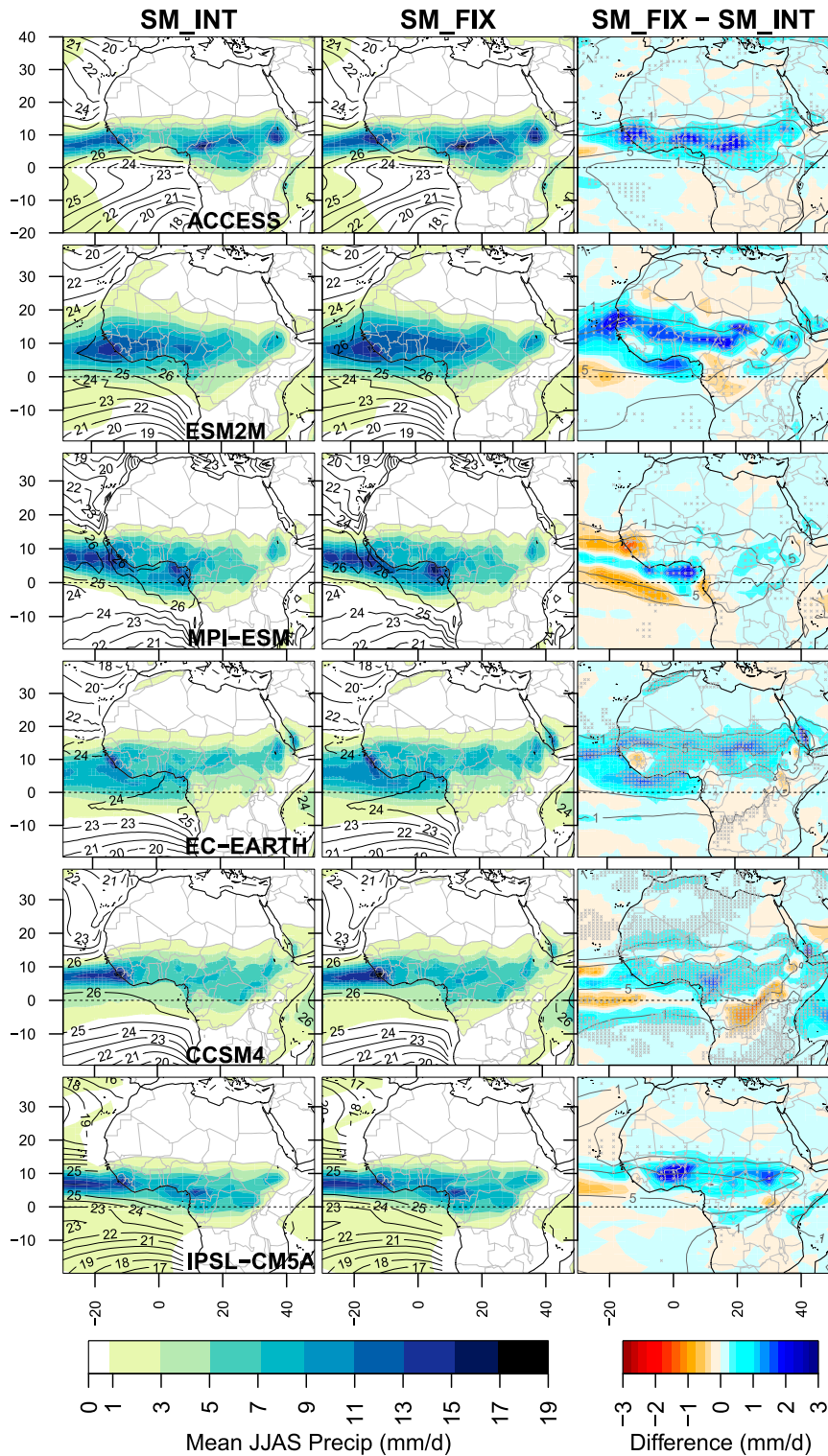


FIG. 2. Mean JJAS precipitation (mm day^{-1}) in (left) SM_INT and (center) SM_FIX simulations over 1971–2000 and (right) SM_FIX – SM_INT difference. The gray contour line over land delineates the 1 mm day^{-1} isohyet. Black contour lines over oceans represent 2-m air temperature. Stippling on the right-hand plots indicates significant SM_FIX – SM_INT differences (at 5%) according to a simple t test. Black contours represent the 1 and 5 mm day^{-1} isohyet from SM_INT for each model.

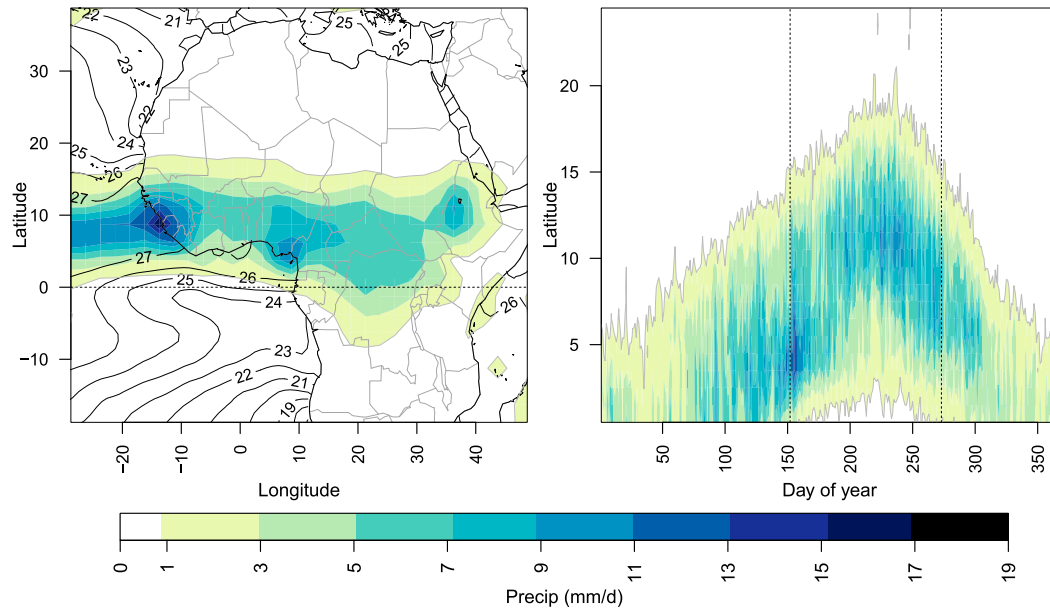


FIG. 3. (left) Mean JJAS precipitation (mm day^{-1}) from monthly GPCP data (Huffman et al. 2009) over 1979–2010 (shading) and mean JJAS sea surface temperatures from the HadISST dataset (Rayner et al. 2003) (contours) and (right) time–latitude view (mean over from -10° to 10°E) of daily mean precipitation (mm day^{-1}) from daily GPCP data over 1996–2010. Gray contour line indicates the 1 mm day^{-1} isohyet.

(or even negative) differences over the northern edge of the climatological monsoon but significant positive differences to both the north and south. Overall, the enhancement of rainy season precipitation in SM_FIX compared to SM_INT is consistent with the increase in rainfall extreme statistics identified in the same simulations in Lorenz et al. (2016; see their Fig. 2).

The general response across models implies that two-way soil moisture–atmosphere interactions in simulation SM_INT reduce rainy season precipitation compared to simulation SM_FIX. However, Fig. 4 reveals more complex impacts on the WAM seasonality. Figure 4 compares mean precipitation in SM_FIX and SM_INT in a time–latitude view. Again, compared to observations (Fig. 3), models differ in their ability to represent the time–latitude behavior of monsoon precipitation, including the monsoon “jump” from the Gulf of Guinea coast to the Sahel in early July (e.g., Sultan and Janicot 2000). Figure 4 also shows that, while JJAS precipitation is enhanced in SM_FIX (consistent with Fig. 2), in at least three models, ACCESS, ESM2M, CCSM4, and to a lesser extent in MPI-ESM and EC-EARTH, premonsoon precipitation (e.g., April–May) near 10°N is reduced in SM_FIX compared to SM_INT. This behavior is more clearly evident in Fig. 5, which, similar to Fig. 2, compares mean precipitation in SM_FIX and SM_INT but for April–May. Figure 5 also shows that in the same models, the reduced early-season

precipitation near 10°N in SM_FIX is associated with enhanced precipitation to the south. Finally, Fig. 4 indicates that some models exhibit changes in precipitation after the peak of the monsoon (October and later), but these changes appear less consistent across models and are not investigated further here. Together, model results in Figs. 2, 4, and 5 demonstrate that soil moisture dynamics affect the mean spatiotemporal dynamics of WAM precipitation.

In the remainder of section 3 we focus on isolating the mechanisms underlying this response. In general, prescription of climatological soil moisture may be expected to impact precipitation mainly by inducing differences in surface–atmosphere turbulent energy fluxes (i.e., the partitioning of available energy between latent and sensible heating); altered turbulent energy fluxes may, in turn, impact precipitation through local land–atmosphere coupling or remotely by altering the surface temperature spatial distribution and thus impacting the large-scale circulation. In the following subsections, we analyze these two terrestrial and atmospheric components. We first analyze how prescribing soil moisture affects land–atmosphere fluxes and surface temperatures.

b. Impacts on surface fluxes and temperatures

Analogous to the difference maps in Fig. 2, Fig. 6 shows the difference in mean JJAS surface latent heat

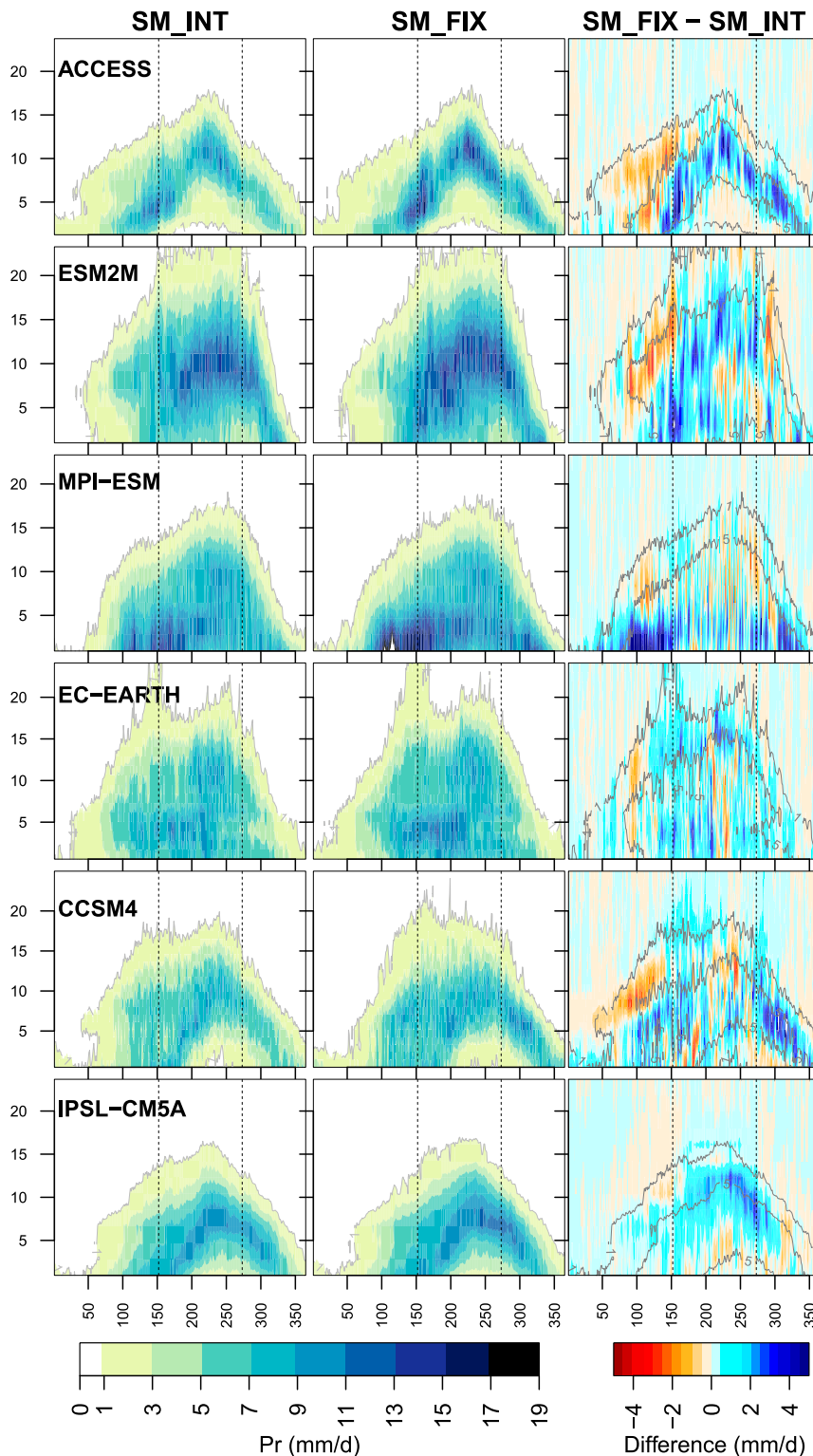


FIG. 4. Time-latitude view (mean over from -10° to 10° E) of daily mean precipitation (mm day^{-1}) in (left) SM_INT and (center) SM_FIX simulations over 1971–2000 and (right) SM_FIX–SM_INT difference (x axis: day of year; y axis: latitude). Vertical dotted bars delimit JJAS (days 152–273). Gray contours indicate the 1 mm day^{-1} isohyet for SM_INT and SM_FIX and the 1 and 5 mm day^{-1} isohyets from SM_INT for each model on the difference plots in (right). Note that for the difference plots, in the interest of readability colors saturate above 5 mm day^{-1} (values reach 10 mm day^{-1} for MPI-ESM near 0° N around day 100).

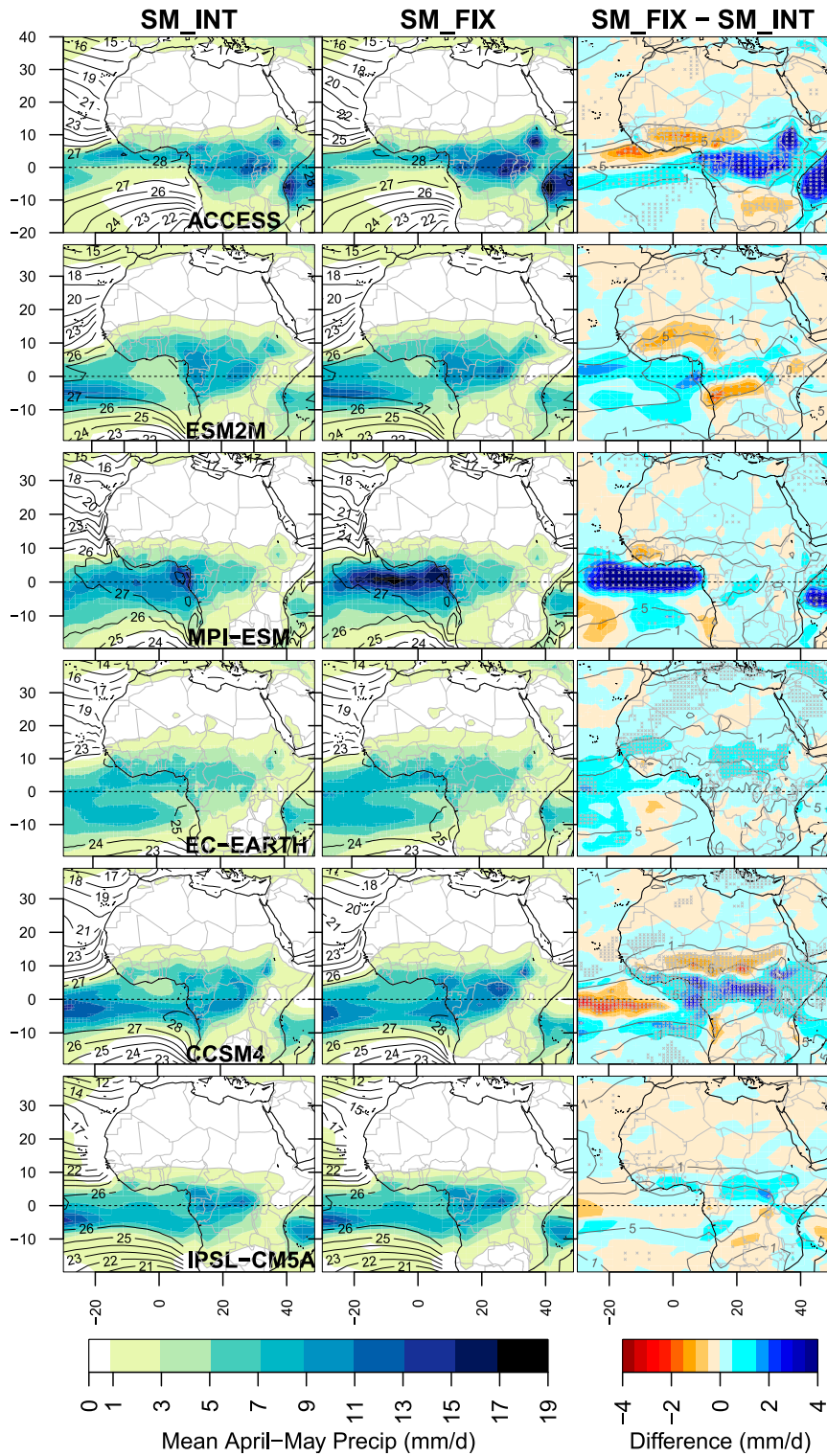


FIG. 5. As in Fig. 2, but for April–May precipitation. Note that for the difference maps, in the interest of readability colors saturate above 4 mm day^{-1} (values reach 8 mm day^{-1} for MPI-ESM over the Gulf of Guinea).

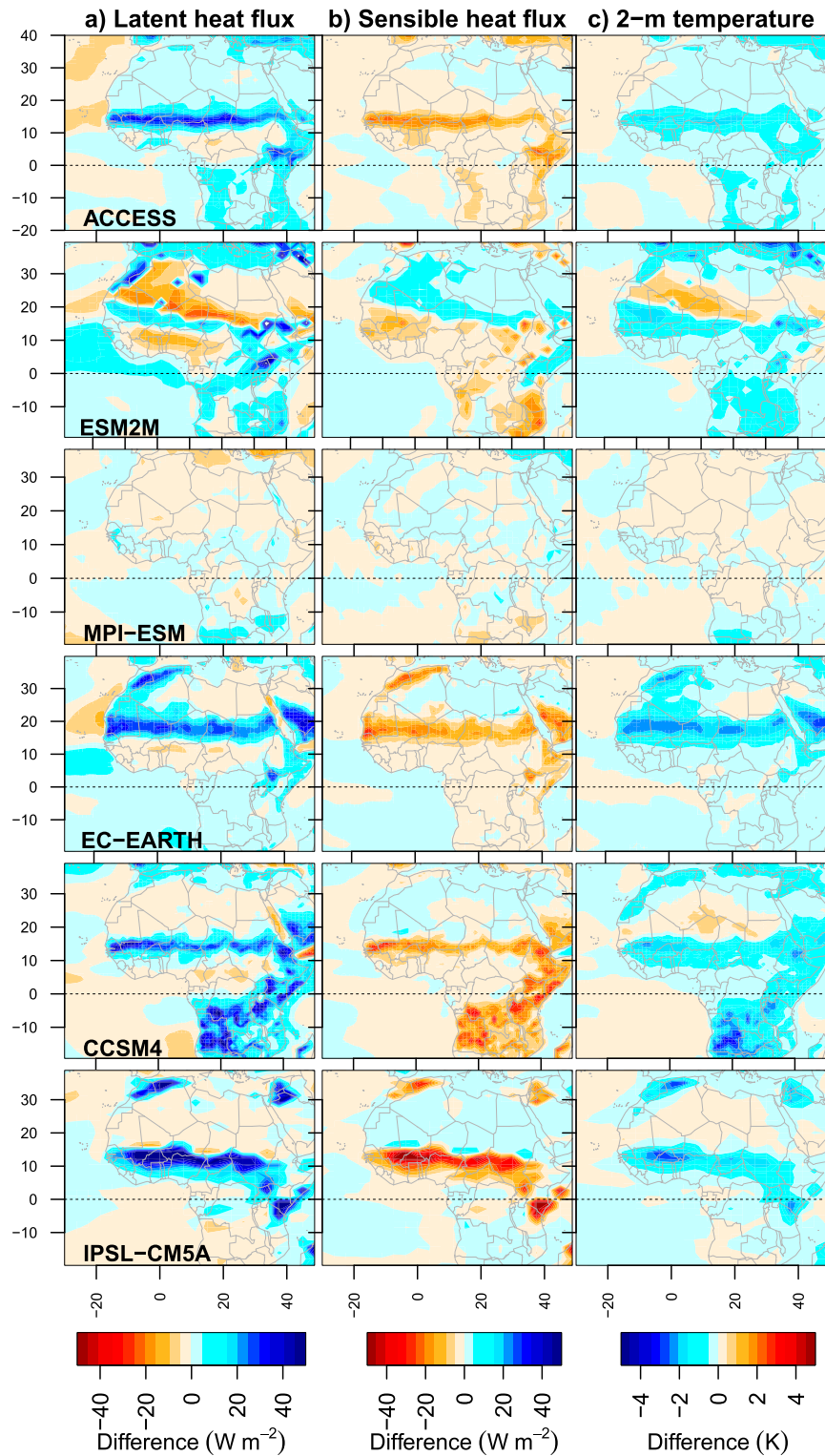


FIG. 6. SM_FIX minus SM_INT difference in mean JJAS (a) surface latent heat flux, (b) sensible heat flux, and (c) 2-m temperature, over 1971–2000. Note that in the interest of readability colors saturate above 50 W m^{-2} (values reach 85 W m^{-2} for the latent heat flux in IPSL-CM5A over the western Sahel). Note the reversed color scale on (c), compared to (a) and (b).

flux, sensible heat flux, and 2-m temperature between SM_FIX and SM_INT in the models. Figure 6a demonstrates that JJAS-mean latent heat flux is enhanced in SM_FIX at the northern edge of the monsoon in all models, except MPI-ESM. The larger latent heat flux in SM_FIX is offset, from a surface energy budget perspective, by reduced sensible heating (Fig. 6b) as well as reduced upwelling longwave radiation (not shown). This is the dominant process responsible for the significant cooling of the surface that can be seen in Fig. 6c over the same part of the domain. Further, Fig. 7 shows that the sign of the response in turbulent heat fluxes and temperature, in contrast to the precipitation response (Fig. 4), is consistent in most models over the course of the monsoon season, depicting an arc of increased latent heat flux, reduced sensible heat flux, and reduced near-surface temperature along the poleward margin of the monsoon.

What causes average changes in the surface energy budget between SM_FIX and SM_INT? We first point out that, as a direct consequence of the experimental design, the larger evapotranspiration in SM_FIX at the margin of the monsoon is not caused by increased precipitation. Indeed, since soil moisture is prescribed in SM_FIX, evapotranspiration does not “see” precipitation. Rather, increased evapotranspiration is a response to the perturbation of soil moisture dynamics (Fig. 1). In general, evapotranspiration is limited either by soil moisture availability in drier regions or by atmospheric demand (influenced by temperature, net radiation, vapor pressure deficit, and wind speed; e.g., Hobbins et al. 2012) in wetter regions. The enhanced evapotranspiration in SM_FIX at the northern edge of the monsoon can be understood as the result of prescribing soil moisture to its climatological value in a soil-moisture-limited evaporative regime: while evapotranspiration in SM_INT is constrained by soil moisture availability and thus the occurrence of rain events to supply soil moisture, in SM_FIX, the prescribed climatological soil water is always available to sustain evapotranspiration even in the absence of rain events (i.e., there are no soil moisture dry downs in SM_FIX). In other words, removing soil moisture interactivity alleviates the soil moisture limitation on evapotranspiration. On the other hand, in SM_INT, the absence of spikes of increased soil moisture after rain events, as occurs in SM_INT, does not lead to a symmetrical decrease in evapotranspiration because climatological soil moisture is generally large enough to sustain similar values of evapotranspiration as in the interactive case. As a result, total evapotranspiration at the northern edge of the monsoon is enhanced in SM_FIX. In a drier, soil-moisture-limited environment soil moisture exhibits

greater daily variability around the seasonal cycle (Fig. 1); the enhancement of evapotranspiration in SM_FIX thus tends to also coincide with the region of greatest difference in soil moisture variability between SM_FIX and SM_INT (Figs. 1 and 6).

Figure 8 illustrates this effect for one grid point in the Sahel for a particular year in the ACCESS model. In SM_INT, evapotranspiration follows the occurrence of rainfall [daily correlation is $r = 0.47$ over July–September (JAS)], whereas in SM_FIX, evapotranspiration appears more independent of precipitation events ($r = 0.13$). Evapotranspiration in SM_FIX actually tends to drop during precipitation events, suggesting evapotranspiration is then energy limited and driven by variations in cloud cover and incident radiation at the surface (daily correlation between evapotranspiration and incoming surface shortwave radiation is $r = 0.48$ over JAS). This difference in evaporative regimes between SM_FIX and SM_INT is also identified in Berg et al. (2015) and is robust across models. On average, the surface latent heat flux in Fig. 8 is $\sim 20 \text{ W m}^{-2}$ greater in SM_FIX than in SM_INT (56.3 compared to 34.5 W m^{-2}), despite soil moisture being comparable for that particular year and model in both simulations. Berg et al. (2014, their Fig. 3) demonstrate this difference at the global scale by comparing simulations SM_FIX and SM_INT from the ESM2M model over the same time period; in dry environments mean evapotranspiration is systematically enhanced in SM_FIX. As can be seen in Fig. 6, this effect is robust across the GLACE-CMIP5 ensemble over West Africa; only MPI-ESM shows little mean change in surface evapotranspiration between the two simulations. This may be linked to biases in the land component of this particular model (see discussion section) and is consistent with the near absence of a JJAS-mean precipitation response in this model in Fig. 2.

Other intermodel differences in Fig. 6 include the particular pattern in ESM2M, with a decrease in evapotranspiration in SM_FIX poleward of the zone of enhanced evapotranspiration (i.e., over the Sahara). Hints of a similar behavior are also noticeable for IPSL-CM5A (although farther to the south). Following Berg et al. (2014), our interpretation of that behavior is that in this region, the climatological values of soil moisture in SM_FIX are too low to support much evapotranspiration; however, following intermittent rain events, appreciable evapotranspiration still occurs in SM_INT so that mean evapotranspiration is eventually larger than in SM_FIX. This effect may be most pronounced in ESM2M because monsoon precipitation extends poleward of 20°N (Figs. 2 and 4). ESM2M also exhibits a slight decrease in evapotranspiration in SM_FIX closer to the Gulf of Guinea coast. This arises from an increase in cloud cover

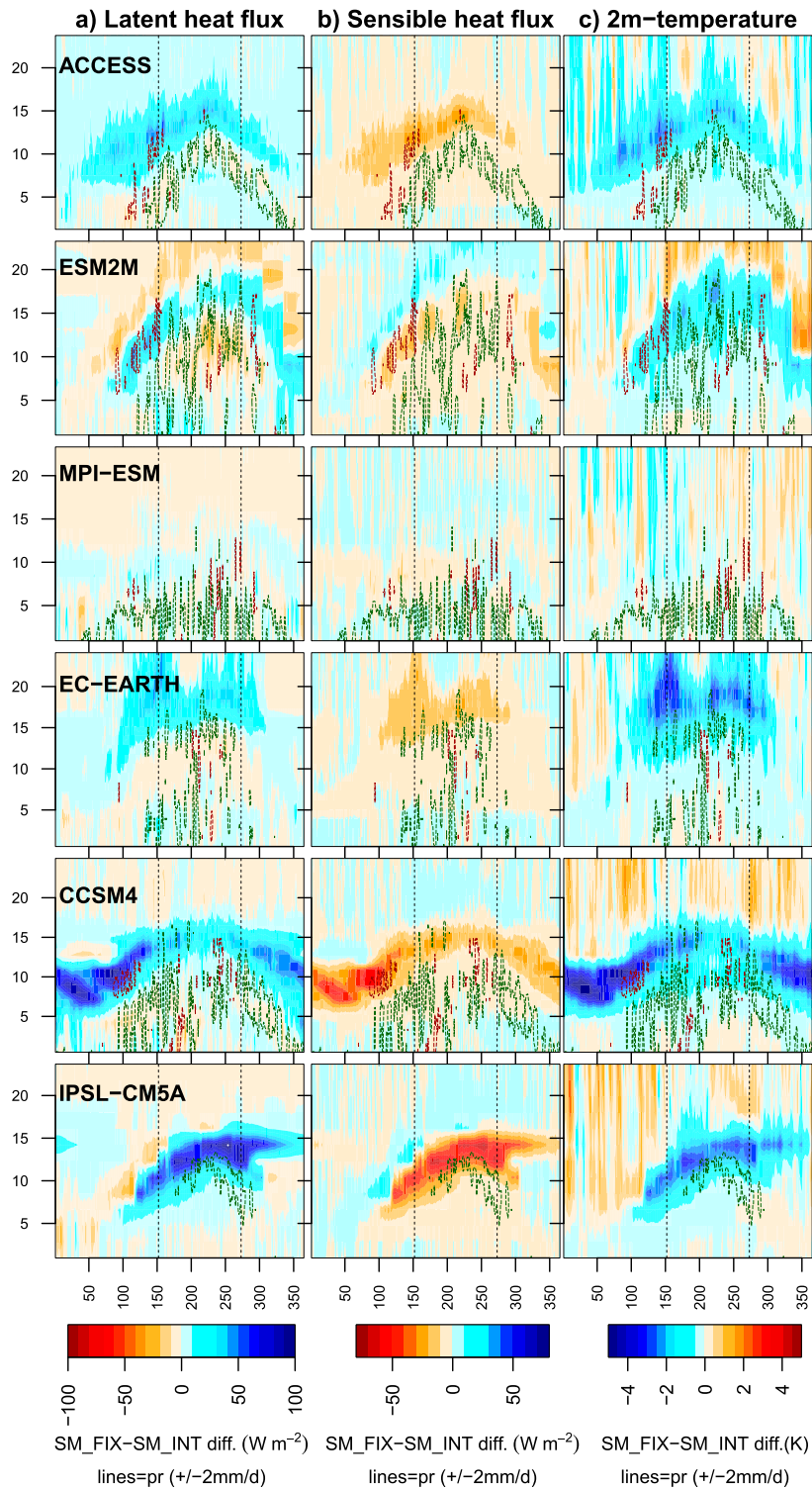


FIG. 7. Time-latitude view (mean over from -10° to 10°E) of (a) difference in mean daily surface latent heat flux (W m^{-2}) between SM_INT and SM_FIX ($\text{SM_FIX} - \text{SM_INT}$) over 1971–2000; (b) as in (a), but for sensible heat flux (W m^{-2}) and (c) 2-m temperature (K). Dashed lines correspond to differences in precipitation (from Fig. 4) greater than $\pm 2 \text{ mm day}^{-1}$ (green: positive; red: negative). Note the reversed color scale on (c), compared to (a) and (b).

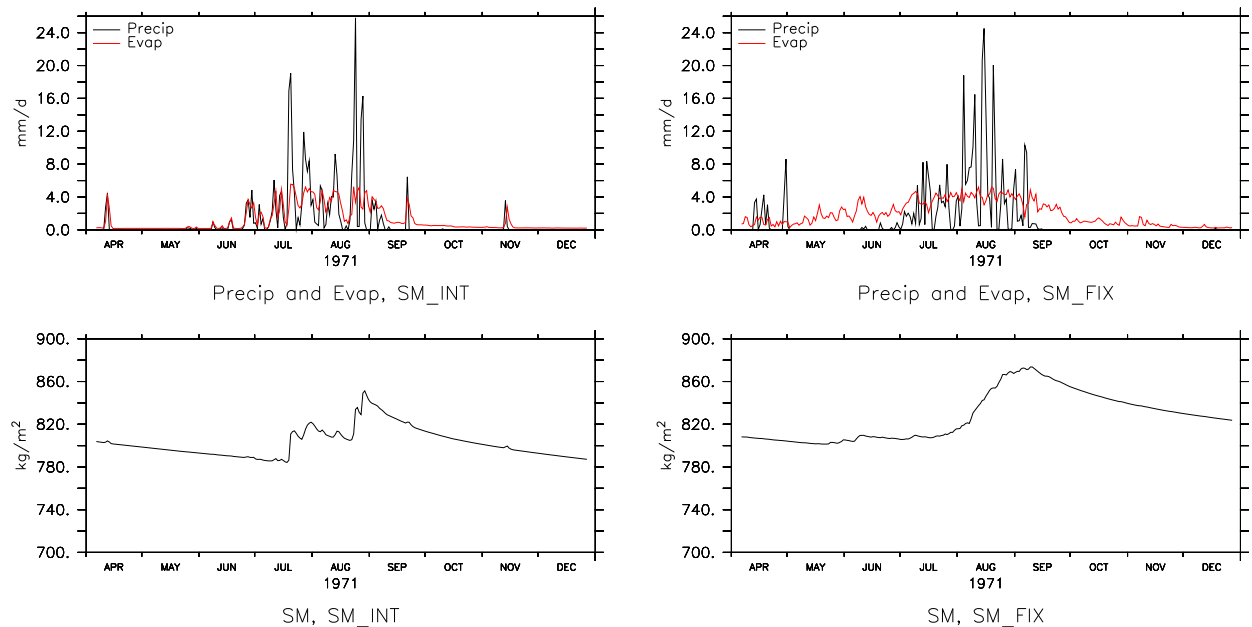


FIG. 8. (top),(left) Precipitation (black) and evapotranspiration (red) over April–September in 1971 in simulation SM_INT from the ACCESS model over one selected pixel in the Sahel (0°E , 14°N); (bottom),(left) total-column soil moisture over the same pixel in the same simulation. (right) As in (left), but in simulation SM_FIX.

and reduction in incoming solar radiation at the surface (evapotranspiration being energy limited in that region). CCSM4 and EC-EARTH also display hints of a cloud-mediated decrease in evapotranspiration in that region.

In the next subsection, we focus on how the changes in surface fluxes and temperatures described above impact precipitation.

c. Impacts on precipitation

As noted above, impacts on rainfall from altered turbulent heat fluxes may occur locally through local land–atmosphere coupling, involving positive or negative impacts of higher evapotranspiration on precipitation (e.g., [Gentine et al. 2013](#)), or remotely through impacts on the large-scale circulation. Careful examination of [Figs. 2](#) and [6](#) reveals that the locus of increased precipitation in JJAS in SM_FIX occurs somewhat equatorward of the increase in surface latent heat flux. [Figure 7](#) further illustrates this: increased evapotranspiration during the core of the rainy season appears poleward of the increased precipitation throughout the seasonal progression of the monsoon. The latitudinal offset between increases in evapotranspiration and precipitation suggests that the processes at play do not simply involve local coupling between increased evapotranspiration in SM_FIX and the precipitation response. On the other hand, [Fig. 7](#) also shows that in models exhibiting reduced precipitation in SM_FIX

during the early part of the season, the change in rainfall is more latitudinally collocated with the change in evapotranspiration. However, these changes are of opposite sign; that is, decreased rainfall on average in SM_FIX is collocated (from a time–latitude perspective) with increased evapotranspiration. This again illustrates that the processes involved are not simple local water recycling. Rather, we now demonstrate how the difference in near-surface temperatures can impact the large-scale circulation in the WAM. Because only the three-dimensional fields from the ESM2M model were available to us, we focus on this model here. While ESM2M displays a particular pattern of evapotranspiration difference between SM_FIX and SM_INT ([Fig. 6](#)), the time–latitude pattern of surface temperature changes is similar to that of other models ([Fig. 7](#)). We will further discuss the applicability of our results to other models in [section 4](#). Given the seasonally contrasting precipitation differences between SM_FIX and SM_INT described in [section 3a](#), we consider the circulation responses for both the early and core monsoon periods.

1) EARLY SEASON

For the early season, we focus on the month of May. [Figures 4](#) and [7](#) show that the ESM2M model is one of the models exhibiting enhanced evapotranspiration, surface cooling, and reduced precipitation at that time (days 120–151 of year) in simulation SM_FIX compared

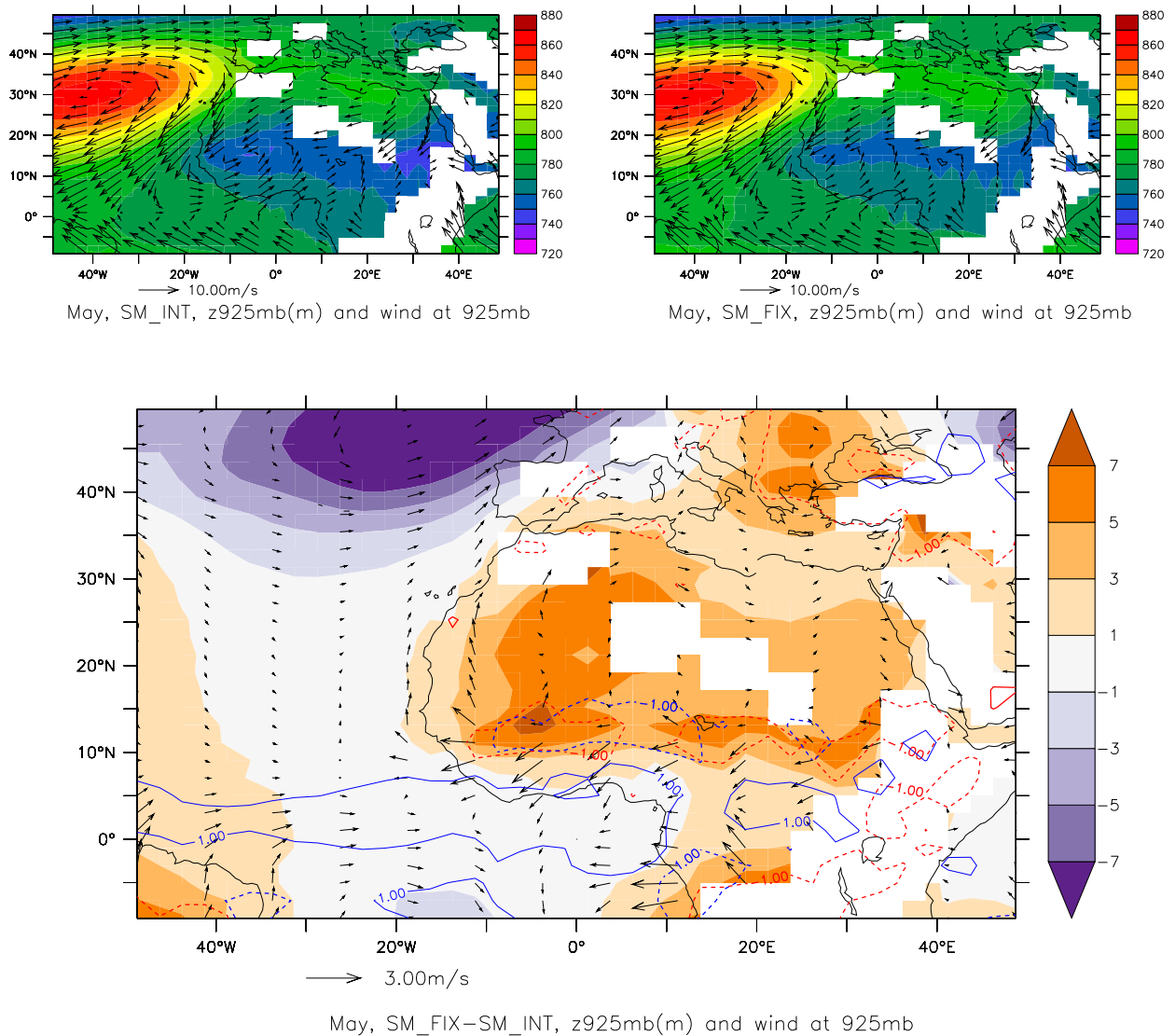


FIG. 9. (top),(left) Mean 925-mb geopotential height (shading; m) and wind (vectors; m s^{-1}) in May in SM_INT, in ESM2M; (right) As in (left), but in SM_FIX. (bottom) SM_FIX – SM_INT difference. Blue and red contours indicate differences in precipitation and temperature, respectively, greater than $\pm 1 \text{ mm day}^{-1}$ or $\pm 1 \text{ K}$ (solid contour: positive difference; dashed contour: negative difference).

to SM_INT. Figure 9 depicts the average low-level circulation in May in both simulations in ESM2M. The cross-equatorial flow characteristic of the WAM is already developed at that time and evident in both simulations, as are the low-level southwesterlies that transport Atlantic moisture inland. However, the relative surface cooling in SM_FIX compared to SM_INT (red dashed lines in Fig. 9, bottom), which is the result of enhanced latent heat flux and reduced sensible heat flux, leads to local positive anomalies in surface pressure (note that positive low-level geopotential height anomalies farther north over the Sahara are not directly associated with surface cooling). These local positive

surface pressure anomalies are associated with anomalous northeasterly flow that opposes the mean southwesterlies. The reduced strength of the monsoon circulation in SM_FIX is associated with a clear dipole of precipitation anomalies, with less precipitation inland, collocated with the region of surface cooling, and increased precipitation over the Gulf of Guinea. In other words, surface cooling in SM_FIX leads to an anomalous high that suppresses the early-season advance of the monsoon. Surface evaporative cooling over 10° – 15° N in SM_FIX may also contribute to enhanced rainfall along the Gulf of Guinea coast at this time of year according to the mechanism discussed recently in

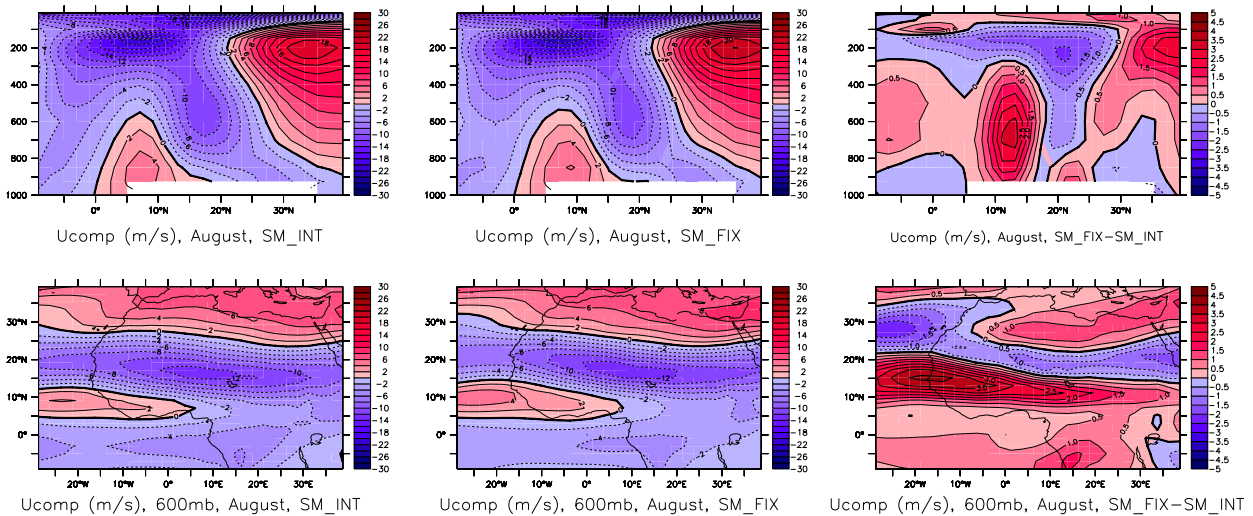


FIG. 10. Mean August zonal wind over 1971–2000 in ESM2M in (left) SM_FIX, (center) SM_INT, and (right) SM_FIX–SM_INT difference. (top) Latitude–pressure view (mean over from -10° to 10° E); (bottom) longitude–latitude view at 600 mb.

Cook (2015): surface cooling around 10° – 15° N is associated with a slightly stronger (i.e., more negative) meridional gradient in midlevel (600 mb; 1 mb = 1 hPa) geostrophic zonal wind between the Gulf of Guinea coast and $\sim 10^{\circ}$ N (not shown), which contributes to reinforcing atmospheric inertial stability near the coast and thus may contribute to enhancing rainfall at those latitudes (Cook 2015). Overall, Fig. 9 implies that soil moisture–atmosphere interactions, as well as the accompanying land drying and warming, are essential for the development of the monsoon circulation at the monsoon onset. Note that in SM_INT, the land region that receives more precipitation than in SM_FIX on average still evaporates less and is warmer than in SM_FIX; despite the greater rainfall this region remains soil moisture limited.

2) CORE SEASON

Here we focus on the month of August, when the monsoon is most developed and most of WAM precipitation occurs. Figure 10 (top) depicts the zonal circulation over West Africa in both simulations for that month. This view reveals well-known features of the WAM circulation, with low-level westerlies bringing moisture from the Atlantic, an easterly wind maximum near 600 mb corresponding to the African easterly jet (AEJ), and another maximum near 200 mb corresponding to the tropical easterly jet. Figure 10 (bottom) focuses on the AEJ over West Africa in both simulations. Difference plots, both on the zonal mean and the longitude–latitude view, reveal a pronounced northward shift of the AEJ in SM_FIX. This northward shift is consistent with the increase in precipitation, as the latitudinal location of the AEJ has long been shown to be

associated with the amount of precipitation over the northern part of West Africa (Newell and Kidson 1984; Rowell et al. 1992; Nicholson and Grist 2001; Grist and Nicholson 2001). Figure 11 further shows that the simulated northward shift of the AEJ follows the change in geostrophic winds, as it is largely mirrored in the calculated changes in geostrophic winds between both simulations. This is consistent with previous analyses indicating that the AEJ has a large geostrophic component and is essentially caused by the presence of a positive (poleward increasing) surface temperature gradient, which, according to the thermal wind relationship, induces easterly shear over the surface monsoon westerlies (Cook 1999).

A mechanism can thus be envisioned by which soil moisture–atmosphere interactions influence precipitation, as depicted in Fig. 12. Figure 12 (top) shows that the position of the jet is roughly associated with the zone of maximum meridional surface temperature gradient in both runs. Surface cooling in SM_FIX over the Sahel leads to a northward shift of the meridional surface temperature gradient; the difference map between both simulations (Fig. 12, bottom) shows that this gradient is enhanced at the northern edge of the area of surface cooling. This change in gradient can be understood more clearly by considering zonal profiles of near-surface temperature in both runs in Fig. 13. One can see the steeper gradient in SM_FIX between 15° and 20° N that results from surface cooling around 15° N. As a result, the AEJ shifts northward in SM_FIX (Fig. 10), which is associated with greater rainfall in the region newly situated south of the AEJ. Previous studies have shown that the AEJ influences Sahel precipitation by

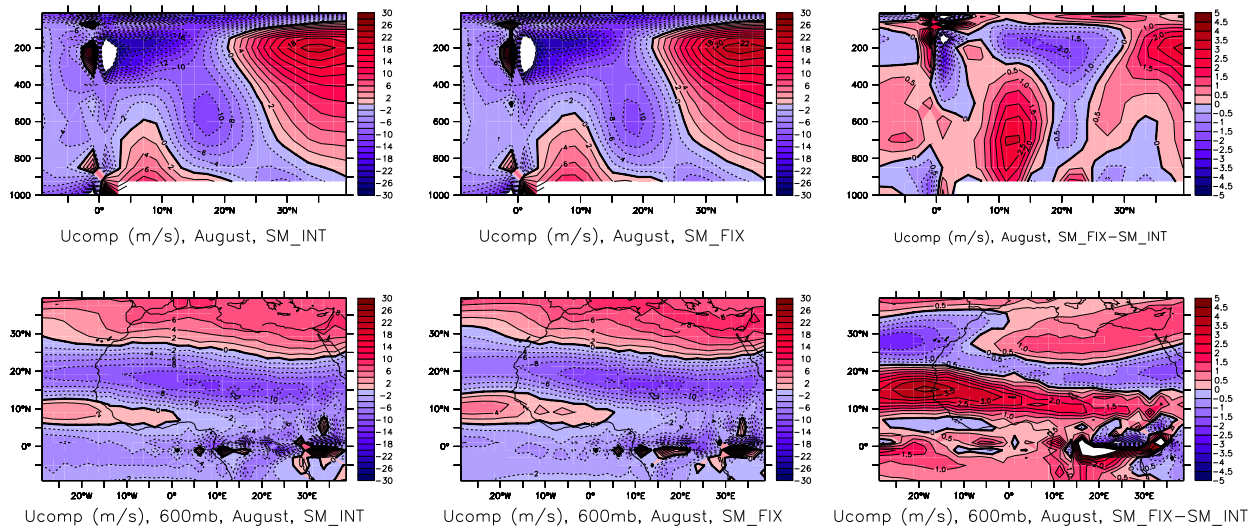


FIG. 11. As in Fig. 10, but for the zonal component of calculated geostrophic wind. Note that this calculation is not valid near the equator.

transporting moisture off the continent, thus increasing moisture divergence over West Africa; the increase in rainfall with a northward displacement (or a weakening) of the AEJ is thus generally interpreted as the result of reduced moisture divergence (Rowell et al. 1992; Cook 1999; Rowell 2003). Figure 12 (bottom) is consistent with this interpretation, as the westerly 600-mb wind anomalies around 15°N are associated with reduced moisture export from the West African region to the Atlantic (note that these anomalies oppose the mean flow but do not correspond to a net reversal of the zonal wind). In our case, in addition to reduced moisture export, the northward shift of the AEJ is also associated with enhanced low-level westerlies in SM_FIX (Fig. 14). This enhances moisture convergence and feeds the simulated increase in precipitation. Following Rowell (2003), we suggest that these enhanced westerlies correspond to a positive feedback mechanism whereby the additional convective heating over the Sahel from enhanced precipitation affects low-level convergence and induces moisture import from the tropical Atlantic. From a dynamical perspective, the strengthened low-level westerlies may also be viewed as a means to achieve vorticity balance, as they advect anticyclonic relative vorticity from the Atlantic high onto the continent to balance the column stretching due to the additional condensational heating around 10°–15°N (Patricola and Cook 2007).

From the above analysis focusing on the simulated monsoon response to prescribed soil moisture climatology, it follows that soil moisture–atmosphere interactions, through their impacts on meridional surface temperature gradients, influence the large-scale zonal

circulation of the WAM. Impacts on surface conditions of soil moisture–atmosphere interactions constrain the latitudinal position of the AEJ and associated precipitation.

4. Discussion

Our results demonstrate pathways by which soil moisture–atmosphere interactions remotely influence the large-scale circulation of the WAM. We show that in dry environments, soil moisture–atmosphere interactions ultimately result in mean drying and warming of the local surface climate, as previously demonstrated in Berg et al. (2014). Our results suggest that in April–May, drying and warming of the land (at the end of the dry season) plays a role in the onset of the monsoon, as precipitation over land is delayed in the absence of soil moisture–atmosphere interactions. This mechanism is consistent with a first-order characterization of the monsoon as a large-scale land–sea breeze, in which the land–sea seasonal warming contrast plays a critical role. During the core of the rainy season, the zonal circulation of the monsoon is found to be sensitive to the impact on surface temperature gradients from soil moisture–atmosphere interactions.

In the following we discuss several aspects related to these results.

a. Role of surface conditions in WAM atmospheric circulation

While the AEJ has long been studied as a prominent feature of the WAM that interacts with many aspects of the monsoon (e.g., African easterly waves), relatively

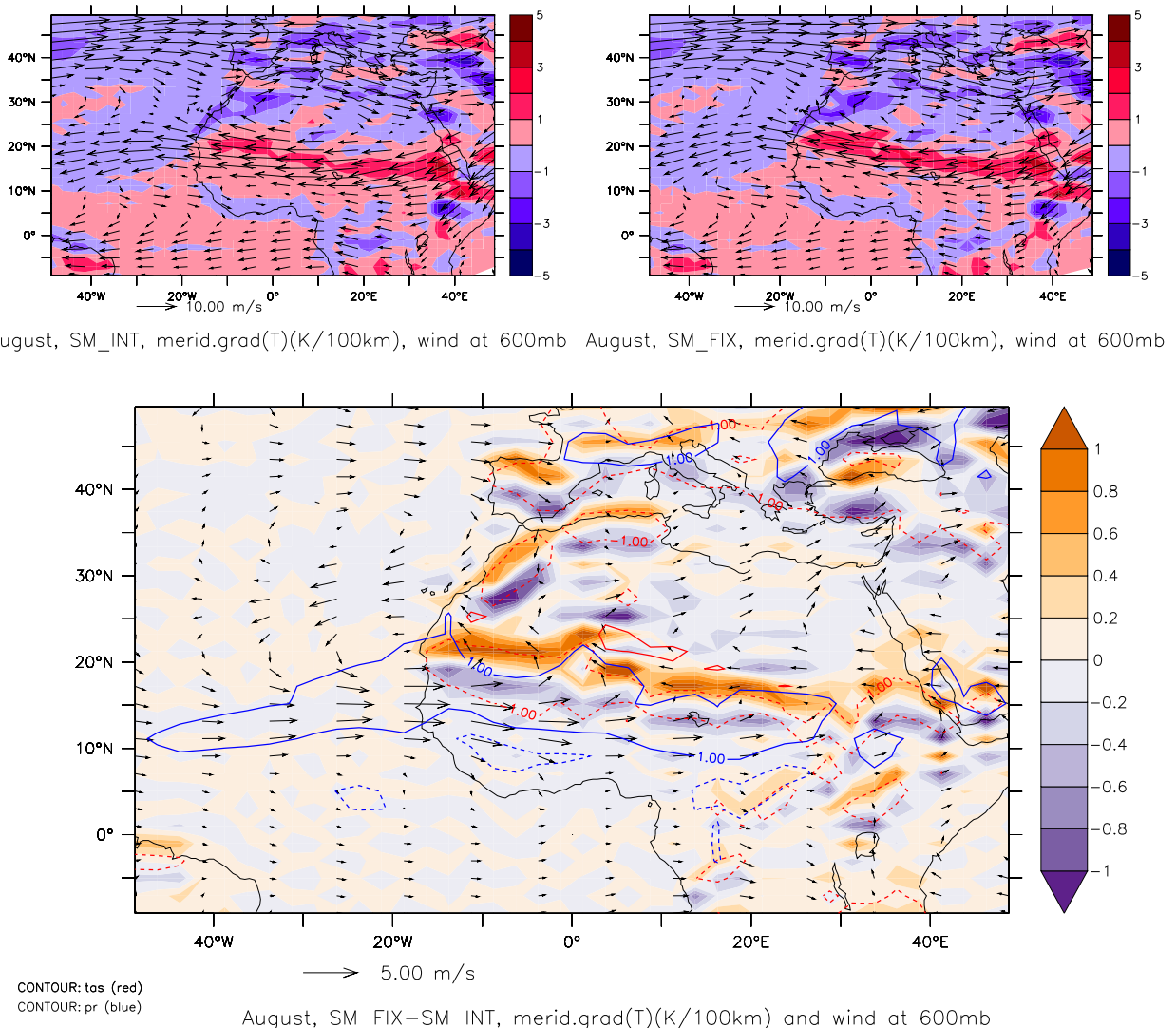


FIG. 12. (top),(left) Mean meridional 2-m temperature gradient [shading; $\text{K} (100 \text{ km})^{-1}$] and 600-mb wind (vectors; m s^{-1}) in August in SM_INT, in ESM2M; (right) as in (left), but in SM_FIX. (bottom) SM_FIX-SM_INT difference. Blue and red contours indicate differences in precipitation and 2-m temperature, respectively, greater than $\pm 1 \text{ mm day}^{-1}$ or $\pm 1 \text{ K}$ (solid contour: positive difference; dashed contour: negative difference).

few studies have focused explicitly on the boundary condition controls on the AEJ. The early work of Cook (1999) showed that the steep, negative meridional soil moisture gradient over West Africa, from the wet areas close to the Gulf of Guinea coast to the dry environment of the Sahara Desert, is essential to maintaining the zone of low-level baroclinicity primarily responsible for the existence of the AEJ. In Cook (1999)'s climate model simulations, this soil water gradient is necessary to generate a temperature gradient sufficient for the AEJ to appear; that is, the positive meridional temperature gradient over West Africa associated with the summertime distributions of solar radiation, SSTs, or clouds

are not large enough to produce the AEJ when homogeneous soil moisture gradients are prescribed. Their results, however, were obtained in highly idealized conditions (e.g., zonally prescribed clouds and SSTs, no diurnal cycle, no orography, and homogeneous albedo). More recently, Wu et al. (2009) investigated surface controls on the structure and maintenance of the AEJ in a more realistic experimental framework. They found that not only soil moisture and evapotranspiration gradients but also the vegetation gradient and orography are essential for the maintenance of the AEJ.

Our results are consistent with the general implications of these earlier studies that meridional surface

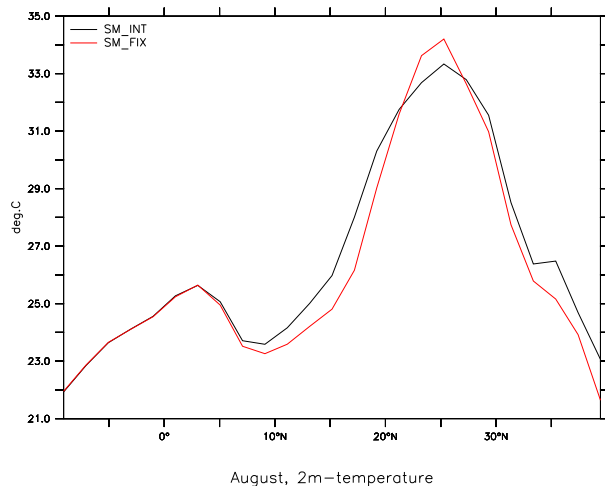


FIG. 13. Mean zonal profile (mean over from -10° to 10° E) of 2-m temperature in SM_INT (red) and SM_FIX (blue) in ESM2M in August over 1971–2000.

moisture gradients contribute to establishing and sustaining the AEJ, and they further show that soil moisture–atmosphere interactions are a key component of this control. These results support the notion of a feedback loop involving precipitation, soil moisture, and the AEJ: increased (decreased) precipitation at Sahelian latitudes is associated with increased (reduced) soil moisture, a northward (southward) shift in the meridional temperature gradient, and a corresponding northward (southward) shift of the AEJ, which further increases (reduces) precipitation (e.g., Rowell et al. 1992). This feedback substantially affects the mean state of the WAM (Fig. 2). Our results are also consistent with a number of studies that find impacts of perturbed surface conditions on precipitation over West Africa involving similar latitudinal shifts in the zonal tropospheric circulation in the context of soil moisture anomalies used to initialize seasonal forecasts (Thiaw and Mo 2005), from changes in the land component of a climate model (Steiner et al. 2009), or from perturbations to the vegetative land cover (e.g., Li et al. 2007) including in the context of paleoclimate (e.g., mid-Holocene) experiments (Patricola and Cook 2008; Rachmayani et al. 2015). Such results underscore the sensitivity of the WAM circulation and precipitation to surface conditions.

It is also worth noting that the near-surface climate effects of prescribing soil moisture are broadly consistent with those associated with irrigation (e.g., Cook et al. 2011). Indeed, like irrigation, we have shown that prescribing soil moisture enhances evapotranspiration and leads to surface cooling in dry

regions. Thus, our results may be relevant to the potential impacts of irrigation in West Africa. For example, Im et al. (2014) and Im and Eltahir (2014) recently showed that developing irrigation over the Sahel has the potential to remotely increase precipitation to the south of the irrigated area through impacts on surface temperature and atmospheric circulation, although their results emphasize more local-scale circulations rather than large-scale features like the AEJ, presumably because of the more spatially limited area of surface perturbation applied in their study. Moreover, irrigation impacts on early-season evapotranspiration and the partitioning of the surface energy budget over India have been shown to dampen the seasonal development of the land–sea warming contrast and reduce early-season monsoon precipitation in that region (Lohar and Pal 1995; Lee et al. 2009; Guimberteau et al. 2012). This behavior is consistent with the relative reduction of early-season reduction of precipitation evident in SM_FIX.

b. Thermodynamic arguments

In our interpretation of the core-season enhancement of rainfall in SM_FIX, we focused on the dynamics of the monsoon to relate changes in surface temperature gradients with zonal circulation changes. We point out that our results are also consistent with studies adopting a more thermodynamic view of monsoonal precipitation. It has long been understood, for instance, that the WAM circulation is more developed and precipitation increases when the meridional gradient of boundary layer moist entropy is greater (e.g., Eltahir and Gong 1996). Figure 15 shows that, on average, this gradient is indeed larger in SM_FIX than in SM_INT in August (Fig. 15a), as moistening along the northern edge of the monsoon (i.e., around 20° N) effectively counteracts local air cooling (Fig. 15b)—both presumably resulting from the increased evapotranspiration and surface cooling in Fig. 6. To the extent that variations in boundary layer entropy are uniquely related to variations in equivalent potential temperature θ_e , Figs. 15c,d are also consistent with Hurley and Boos (2013), who show that positive monsoon precipitation anomalies are associated with enhanced low-level (subcloud) θ_e collocated with as well as slightly poleward of the climatological θ_e maximum. Their results emphasize the importance of low-level moisture anomalies poleward of the precipitation peak for the variability of subcloud θ_e and thus for the interannual variability of monsoons. Furthermore, Su and Neelin (2005) have noted the role of ventilation of the West African monsoon by dry (low moist entropy) air originating over the Sahara. We speculate that enhanced low-level moistening in SIM_FIX moderates the dry air inflow along the

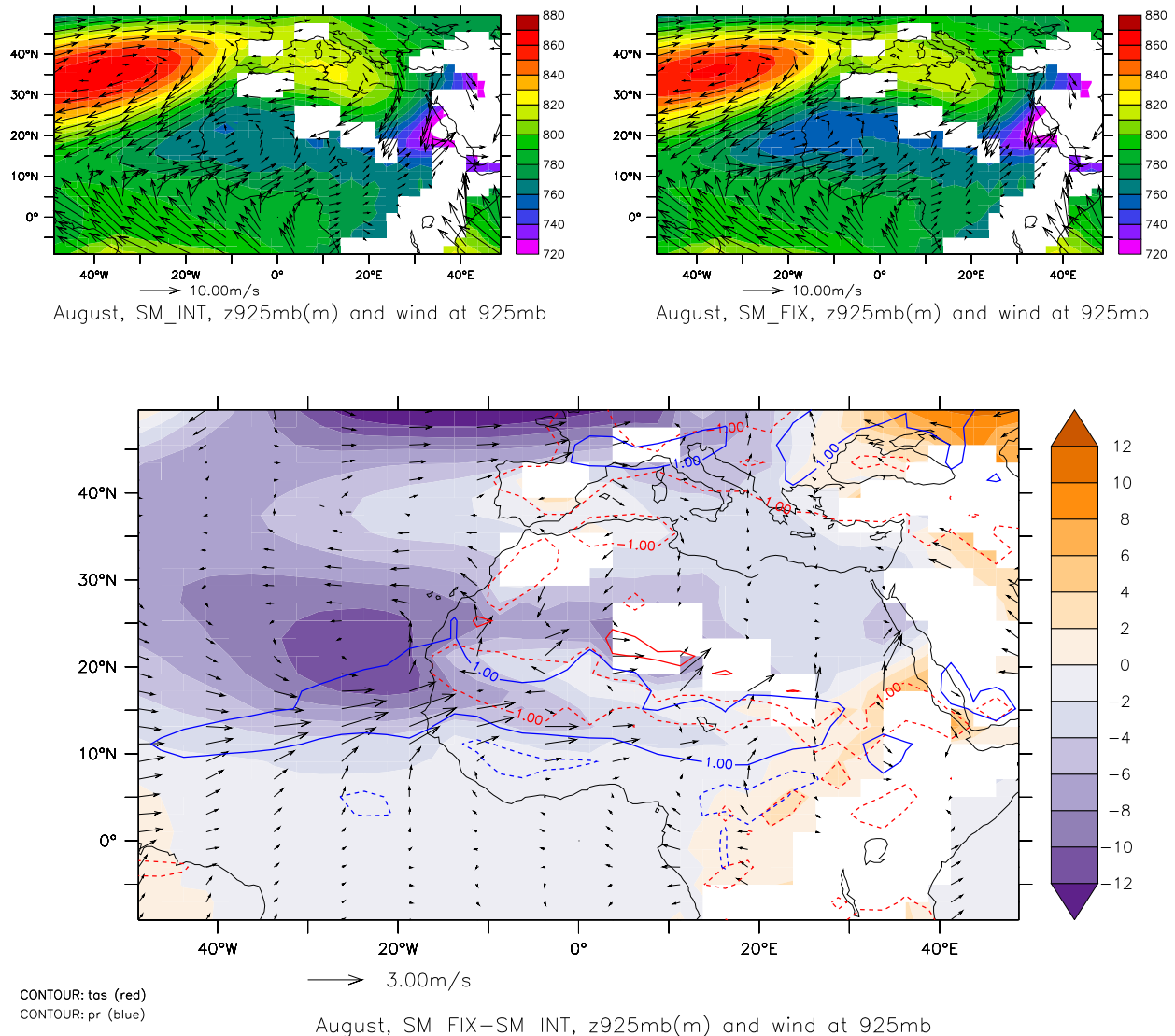


FIG. 14. As in Fig. 9, but for August.

poleward margin of the monsoon and that this might contribute to higher rainfall in the monsoon.

c. Protocol uncertainties

The aim of prescribing soil moisture in SM_FIX in the GLACE-CMIP5 protocol is to disable feedbacks to the atmosphere associated with soil moisture variability. As described in section 3b, prescribing climatological soil moisture in SM_FIX leads to an enhanced climatological mean latent heat flux in dry regions. This is essentially because of the lack of soil moisture dry-down events in SM_FIX. In that sense, the interactivity and (mean) availability of soil moisture appear intrinsically linked: in dry regions, soil moisture interactivity reduces overall soil moisture availability compared to

prescribed soil moisture. In other words, because of the nonlinearity of the soil moisture–evapotranspiration relationship, changes in soil moisture variability eventually impact mean evapotranspiration. It is worth noting, however, that this effect may depend on how soil moisture is overridden in the prescribed case. Admittedly, the choice of soil moisture values with which to override soil moisture in the prescribed simulation is somewhat arbitrary, as there is no clear physical guidance regarding what noninteractive soil moisture should be.

While imposing a climatological seasonal cycle is intuitive—in a sense, it is analogous to forcing climate models with climatological SSTs—other alternatives could be considered. Some prior studies, for instance,

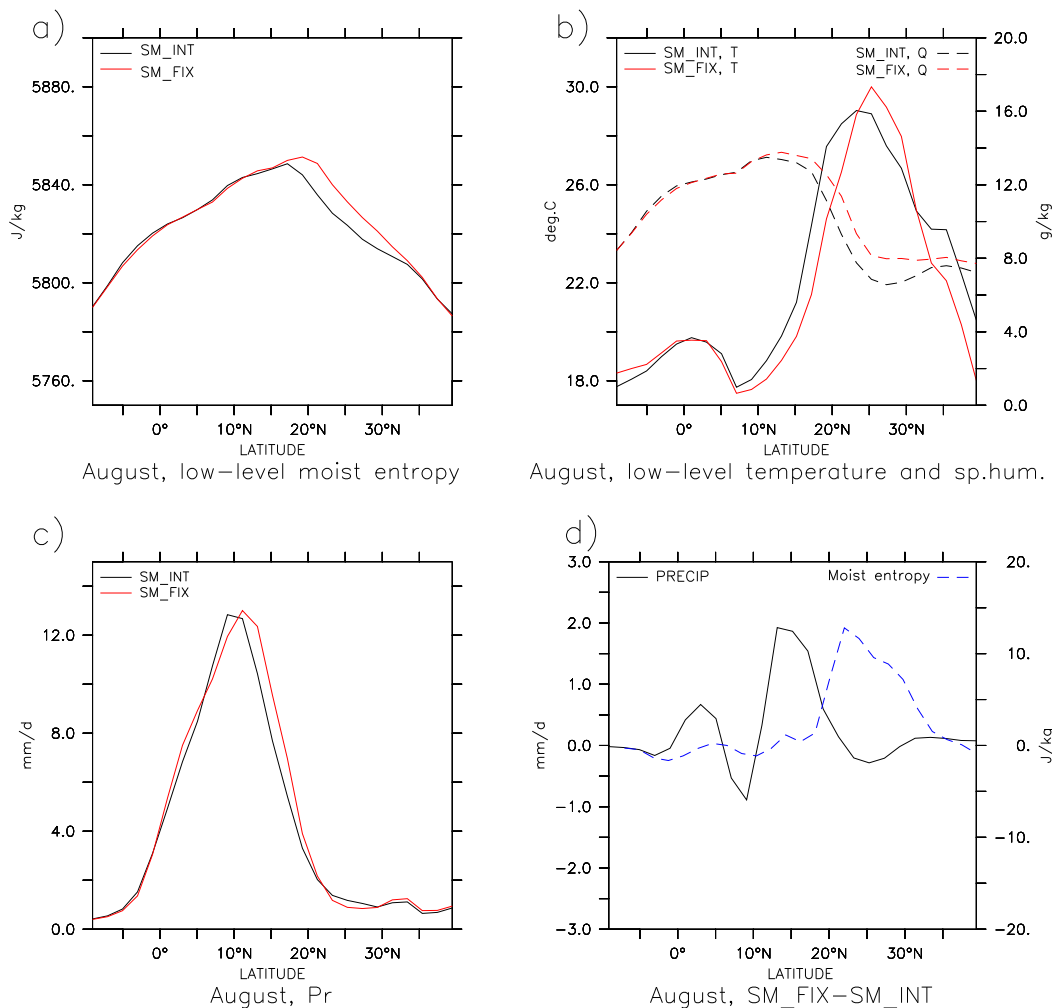


FIG. 15. Mean August zonal profiles in SM_INT and SM_FIX (mean over from -10° to 10° E) of (a) low-level moist entropy (mean between 1000- and 850-mb model levels), (b) low-level air temperature T and humidity Q , (c) precipitation, and (d) SM_FIX-SM_INT difference in profiles of precipitation and moist entropy.

have used constant field capacity to override soil moisture (Cook et al. 2006). In the first GLACE experiment (GLACE-1; Koster et al. 2004), full daily soil moisture time series from the interactive runs were used to override soil moisture in the prescribed simulations. Compared to prescribing climatological values, this approach similarly severs the two-way coupling between soil moisture and the atmosphere but also retains full daily and interannual variability in soil moisture, albeit decoupled from the atmosphere. It is unclear what impacts such a protocol, if applied to the transient climate change simulations in GLACE-CMIP5, would have on mean surface fluxes and climate. Analysis of GLACE-1 simulations with ESM2M suggests that application of this protocol also enhances mean seasonal evapotranspiration (not shown). Overall, because of the

nonlinearity of the relationship between soil moisture and evapotranspiration, we speculate that any protocol overriding soil moisture will ultimately have some impact on mean evapotranspiration and the water availability to the atmosphere. We note here that, within the limited model ensemble used in this experiment, there seems to be no correlation between the different model responses in our analysis and the slightly different ways soil moisture were prescribed in the models; models that used a time step scale, a daily climatology, or a monthly climatology of soil moisture (e.g., ACCESS, IPSL-CM5A, and ESM2M, respectively) display similar behaviors.

As discussed in Berg et al. (2014), another plausible approach to disable soil moisture-atmosphere interactions is to override land surface evapotranspiration

(e.g., Koster et al. 2000; Reale and Dirmeyer 2002; Giannini et al. 2003; Schubert et al. 2004). This approach also disables feedbacks to the atmosphere from soil moisture variability. However, it is conceptually different from the GLACE-CMIP5 protocol in that, in addition to removing evapotranspiration variability due to soil moisture, it removes any variability due to atmospheric controls on evapotranspiration, which are still present in the GLACE-CMIP5 experiments. The impacts on surface climate may thus be different. Reale and Dirmeyer (2002), for instance, report widespread cooling in the Northern Hemisphere from prescribing the seasonal cycle of evapotranspiration efficiency (i.e., the ratio of actual to potential evapotranspiration). This is associated in their simulations with a general southward shift of the ITCZ and reduced monsoon precipitation over West Africa. This underscores how the effects of disabling soil moisture–atmosphere interactions may depend on the experimental protocol. Overall, we emphasize that analyzing the impacts of soil moisture variability on surface climate by comparing interactive versus climatological–soil moisture simulations is not strictly equivalent to isolating the role of soil moisture–atmosphere interactions; the former represents a particular protocol to achieve insight into the more conceptual notion of the latter (Berg et al. 2014).

d. Model uncertainties

With the exception of MPI-ESM, all of the GLACE-CMIP5 models show a consistent response of surface energy fluxes and temperatures over West Africa to soil moisture variability (Figs. 6 and 7). The absence of response in MPI-ESM is consistent with previous analysis of this model showing the weakest influence of soil moisture variability on surface climate across the GLACE-CMIP5 ensemble (not shown). One reason for this is that many of the largest impacts of soil moisture variability in GLACE-CMIP5 occur in arid regions, where bare ground evaporation is a large component of total evapotranspiration; the differences in mean JJAS evapotranspiration in Fig. 6 are in fact mostly due to changes in soil evaporation (not shown). However, the version of MPI-ESM used in GLACE-CMIP5 includes a bucket model for soil moisture that largely underestimates soil evaporation in dry regions. This underestimation arises because, before bare soil evaporation can occur, the bucket must fill entirely so that some water is available in the upper 10 cm of the soil column (Hagemann and Stacke 2015). These conditions are seldom met in arid regions. In particular, soil evaporation is close to zero in MPI-ESM over West Africa. This underestimation appears to be compensated by a larger evaporation from water intercepted by the

canopy as well as a skin layer on the ground. Such water reservoirs are not overridden in GLACE-CMIP5 and continue to respond interactively to precipitation in SM_FIX in MPI-ESM. Thus, because of the bias in soil evaporation and the specificities of the land model in MPI-ESM, overriding soil moisture in this model barely affects evapotranspiration mean and variability, and subsequently surface climate, as in other models.

Given the availability of pressure-level data for ESM2M, we have focused on that model for the analysis of the circulation response to perturbed surface conditions. Given the consistency across models of the time–latitude pattern of precipitation response in relation to evapotranspiration and surface temperature changes during the core season (Figs. 4 and 7), we reason that similar processes to the ones described in section 3 operate in other models. Of course, not all models may reflect similar sensitivity of the monsoon circulation to surface conditions, and more generally, models exhibit considerable spread in the strength of simulated land–atmosphere coupling (e.g., Koster et al. 2004; Guo et al. 2006). Different atmospheric responses to local cooling/moistening along the poleward edge of the monsoon may also come into play. For instance, we speculate that the weaker precipitation response seen in CCSM4 (Fig. 2) could be due to a negative feedback of surface cooling on precipitation, as documented in similar soil moisture experiments with a previous version of the same model (CCSM3) by Cook et al. (2006), in a similar semiarid environment (South Africa); they show that local cooling in that model leads to large-scale subsidence that impedes convective precipitation. The early-season impact described in section 3a is not as consistently simulated across models and may consequently be more uncertain. We speculate that model-to-model differences in early-season precipitation responses may stem from a combination of different early-season evapotranspiration changes (Fig. 7a) with different mean monsoon seasonality (Fig. 4); models like EC-EARTH and IPSL-CM5A that do not exhibit precipitation changes in the early season indeed show little change in surface energy fluxes and temperature in the first place (EC-EARTH), and/or the simulated monsoon onset occurs late enough to be relatively insensitive to such changes (IPSL-CM5A).

GLACE-CMIP5 is a targeted, idealized experiment designed to investigate the role of soil moisture variability, as well as long-term mean soil moisture changes, on surface climate. This role is inferred by comparing model simulations with different soil moisture configurations. We do not assess the realism of the different model responses by explicitly evaluating the control (SM_INT) simulations against observations (as noted in

section 3, model simulations of the WAM in general suffer from numerous shortcomings). Rather, we draw on the consistency of the model responses to support the plausibility of the simulated effects. Along these lines, we emphasize that the model responses to soil moisture variability highlighted in our analysis—both early- and core-season effects—involve feedbacks on the large-scale monsoon circulation; these processes are arguably more reliably simulated in coarse-resolution climate models than local or mesoscale soil moisture–convection feedbacks, which are not yet fully understood from an observational and theoretical perspective (Findell et al. 2011; Taylor et al. 2012; Froidevaux et al. 2014; Guillod et al. 2015) and are questionably represented in climate models (Taylor et al. 2012, 2013). The planned inclusion of GLACE-type simulations in CMIP6 [in the Land Surface Model Intercomparison Project (LSMIP)] should allow for the investigation of these large-scale soil moisture–atmosphere effects, and the associated uncertainties, with a larger suite of models, over West Africa in particular but in other regions as well.

5. Conclusions

By comparing an ensemble of climate model simulations with and without interactive soil moisture, we demonstrate the contribution of soil moisture–atmosphere interactions to the seasonality and distribution of simulated precipitation in the West African monsoon. In five of the six models analyzed, core-season (e.g., August) monsoon precipitation is ultimately reduced when soil moisture is interactive rather than prescribed to the climatological seasonal cycle. On the other hand, in at least half of the models analyzed, early-season (e.g., May) precipitation is enhanced when soil moisture is interactive. We find that the processes underlying these responses involve remote impacts of soil moisture variability on the large-scale circulation. In dry environments such as the northern edge of the monsoon (throughout its seasonal progression), interactive soil moisture leads to drier and warmer conditions, on average, in all but one model analyzed; this warming then impacts the large-scale monsoon circulation. During the core of the monsoon season, this warming affects the overall steepness of the meridional surface temperature gradient and the location of the steepest gradient. This in turn shifts the African easterly jet to the south, reducing precipitation at the poleward edge of the monsoon. Early in the season, surface warming appears essential to the land–sea warming contrast buildup leading to the initial inland excursion of WAM. The additional warming in the interactive soil moisture experiment promotes earlier onset of the monsoon season. These results highlight the role of soil moisture–atmosphere interactions

in shaping large-scale, seasonal aspects of the West African monsoon.

Projections of future precipitation changes over West Africa remain uncertain in current-generation climate models. A robust feature of these projections across models consists of a delay in the seasonal cycle of the monsoon (Biasutti 2013), yet the physical mechanisms underlying this response remain to be elucidated. The present study has identified fundamental impacts of soil moisture–atmosphere interactions on monsoon precipitation, in terms of both mean behavior and seasonality. A question thus raised is how soil moisture–atmosphere interactions may affect the projected changes in the WAM with climate change; this will be the focus of future analysis of the GLACE-CMIP5 simulations.

Acknowledgments. A. B. acknowledges support of NSF Postdoctoral Fellowship AGS-1331375 and B. R. L. acknowledges support of NSF AGS-1505198. We thank Tom Delworth and Spencer Hill for their comments on an earlier version of this manuscript. We thank participants of the GLACE-CMIP5 experiment and members of the corresponding modeling groups for providing simulation outputs from their respective models. GLACE-CMIP5 was sponsored by GEWEX [World Climate Research Programme (WCRP)] and ILEAPS [Integrated Geosphere–Biosphere Programme (IGBP)] projects and coordinated by ETH Zurich. The GLACE-CMIP5 data is hosted and managed at ETH Zurich and is available upon request (see <http://www.iac.ethz.ch/GLACE-CMIP>, subject to agreement of the respective modeling groups).

REFERENCES

- Bader, J., and M. Latif, 2003: The impact of decadal-scale Indian Ocean sea surface temperature anomalies on Sahelian rainfall and the North Atlantic Oscillation. *Geophys. Res. Lett.*, **30**, 2169, doi:10.1029/2003GL018426.
- Berg, A., B. Lintner, K. Findell, S. Malyshev, P. Loikith, and P. Gentile, 2014: Impacts of soil moisture–atmosphere interactions on surface temperature distribution. *J. Climate*, **27**, 7976–7993, doi:10.1175/JCLI-D-13-00591.1.
- , and Coauthors, 2015: Interannual coupling between summertime surface temperature and precipitation over land: Processes and implications for climate change. *J. Climate*, **28**, 1308–1328, doi:10.1175/JCLI-D-14-00324.1.
- Biasutti, M., 2013: Forced Sahel rainfall trends in the CMIP5 archive. *J. Geophys. Res. Atmos.*, **118**, 1613–1623, doi:10.1002/jgrd.50206.
- , and A. H. Sobel, 2009: Delayed Sahel rainfall and global seasonal cycle in a warmer climate. *Geophys. Res. Lett.*, **36**, L23707, doi:10.1029/2009GL041303.
- Cook, B. I., G. B. Bonan, and S. Levis, 2006: Soil moisture feedbacks to precipitation in southern Africa. *J. Climate*, **19**, 4198–4206, doi:10.1175/JCLI3856.1.

- , M. J. Puma, and N. Y. Krakauer, 2011: Irrigation induced surface cooling in the context of modern and increased greenhouse gas forcing. *Climate Dyn.*, **37**, 1587–1600, doi:[10.1007/s00382-010-0932-x](https://doi.org/10.1007/s00382-010-0932-x).
- Cook, K. H., 1999: Generation of the African easterly jet and its role in determining West African precipitation. *J. Climate*, **12**, 1165–1184, doi:[10.1175/1520-0442\(1999\)012<1165:GOTAEJ>2.0.CO;2](https://doi.org/10.1175/1520-0442(1999)012<1165:GOTAEJ>2.0.CO;2).
- , 2015: Role of inertial instability in the West African monsoon jump. *J. Geophys. Res. Atmos.*, **120**, 3085–3102, doi:[10.1002/2014JD022579](https://doi.org/10.1002/2014JD022579).
- Eltahir, E. A. B., and C. Gong, 1996: Dynamics of wet and dry years in West Africa. *J. Climate*, **9**, 1030–1042, doi:[10.1175/1520-0442\(1996\)009<1030:DOWADY>2.0.CO;2](https://doi.org/10.1175/1520-0442(1996)009<1030:DOWADY>2.0.CO;2).
- Findell, K. L., P. Gentine, B. Lintner, and C. Kerr, 2011: Probability of afternoon precipitation in eastern United States and Mexico enhanced by high evaporation. *Nat. Geosci.*, **4**, 434–439, doi:[10.1038/ngeo1174](https://doi.org/10.1038/ngeo1174).
- Folland, C. K., D. E. Parker, and T. N. Palmer, 1986: Sahel rainfall and worldwide sea temperatures 1901–85. *Nature*, **320**, 602–607, doi:[10.1038/320602a0](https://doi.org/10.1038/320602a0).
- Froidevaux, P., L. Schlemmer, J. Schmidli, W. Langhans, and C. Schär, 2014: Influence of the background wind on the local soil moisture–precipitation feedback. *J. Atmos. Sci.*, **71**, 782–799, doi:[10.1175/JAS-D-13-0180.1](https://doi.org/10.1175/JAS-D-13-0180.1).
- Gentine, P., A. A. M. Holtslag, F. D’Andrea, and M. Ek, 2013: Surface and atmospheric controls on the onset of moist convection over land. *J. Hydrometeorol.*, **14**, 1443–1462, doi:[10.1175/JHM-D-12-0137.1](https://doi.org/10.1175/JHM-D-12-0137.1).
- Giannini, A., R. Saravanan, and P. Chang, 2003: Oceanic forcing of Sahel rainfall on interannual to interdecadal time scales. *Science*, **302**, 1027–1030, doi:[10.1126/science.1089357](https://doi.org/10.1126/science.1089357).
- , S. Salack, T. Lodoun, A. Ali, A. T. Gaye, and O. Ndiaye, 2013: A unifying view of climate change in the Sahel linking intra-seasonal, interannual and longer time scales. *Environ. Res. Lett.*, **8**, 024010, doi:[10.1088/1748-9326/8/2/024010](https://doi.org/10.1088/1748-9326/8/2/024010).
- Grist, J. P., and S. E. Nicholson, 2001: A study of the dynamic factors influencing the interannual variability of rainfall in the West African Sahel. *J. Climate*, **14**, 1337–1359, doi:[10.1175/1520-0442\(2001\)014<1337:ASOTDF>2.0.CO;2](https://doi.org/10.1175/1520-0442(2001)014<1337:ASOTDF>2.0.CO;2).
- Guillob, B. P., B. Orłowski, D. G. Miralles, A. J. Teuling, and S. I. Seneviratne, 2015: Reconciling spatial and temporal soil moisture effects on afternoon rainfall. *Nat. Commun.*, **6**, 6443, doi:[10.1038/ncomms7443](https://doi.org/10.1038/ncomms7443).
- Guimberteau, M., K. Laval, A. Perrier, and J. Polcher, 2012: Global effect of irrigation and its impact on the onset of the Indian summer monsoon. *Climate Dyn.*, **39**, 1329–1348, doi:[10.1007/s00382-011-1252-5](https://doi.org/10.1007/s00382-011-1252-5).
- Guo, Z., and Coauthors, 2006: GLACE: The Global Land–Atmosphere Coupling Experiment. Part II: Analysis. *J. Hydrometeorol.*, **7**, 611–625, doi:[10.1175/JHM511.1](https://doi.org/10.1175/JHM511.1).
- Haarsma, R. J., F. Selten, B. van den Hurk, W. Hazeleger, and X. Wang, 2009: Drier Mediterranean soils due to greenhouse warming bring easterly winds over summertime central Europe. *Geophys. Res. Lett.*, **36**, L04705, doi:[10.1029/2008GL036617](https://doi.org/10.1029/2008GL036617).
- Hagemann, S., and T. Stacke, 2015: Impact of the soil hydrology scheme on simulated soil moisture memory. *Climate Dyn.*, **44**, 1731–1750, doi:[10.1007/s00382-014-2221-6](https://doi.org/10.1007/s00382-014-2221-6).
- Held, I. M., T. L. Delworth, J. Lu, K. Findell, and T. R. Knutson, 2005: Simulation of Sahel drought in the 20th and 21st centuries. *Proc. Natl. Acad. Sci. USA*, **102**, 17891–17896, doi:[10.1073/pnas.0509057102](https://doi.org/10.1073/pnas.0509057102).
- Hobbins, M., A. Wood, D. Streubel, and K. Werner, 2012: What drives the variability of evaporative demand across the conterminous United States? *J. Hydrometeorol.*, **13**, 1195–1214, doi:[10.1175/JHM-D-11-0101.1](https://doi.org/10.1175/JHM-D-11-0101.1).
- Hoerling, M. P., J. W. Hurrell, J. Eischeid, and A. S. Phillips, 2006: Detection and attribution of twentieth-century northern and southern African monsoon change. *J. Climate*, **19**, 3989–4008, doi:[10.1175/JCLI3842.1](https://doi.org/10.1175/JCLI3842.1).
- Huffman, G. J., R. F. Adler, D. T. Bolvin, and G. Gu, 2009: Improving the global precipitation record: GPCP version 2.1. *Geophys. Res. Lett.*, **36**, L17808, doi:[10.1029/2009GL040000](https://doi.org/10.1029/2009GL040000).
- Hurley, J. V., and W. R. Boos, 2013: Interannual variability of monsoon precipitation and local subcloud equivalent potential temperature. *J. Climate*, **26**, 9507–9527, doi:[10.1175/JCLI-D-12-00229.1](https://doi.org/10.1175/JCLI-D-12-00229.1).
- Im, E.-S., and E. A. B. Eltahir, 2014: Enhancement of rainfall and runoff upstream from irrigation location in a climate model of West Africa. *Water Resour. Res.*, **50**, 8651–8674, doi:[10.1002/2014WR015592](https://doi.org/10.1002/2014WR015592).
- , M. P. Marcella, and E. A. B. Eltahir, 2014: Impact of potential large-scale irrigation on the West African monsoon and its dependence on location of irrigated area. *J. Climate*, **27**, 994–1009, doi:[10.1175/JCLI-D-13-00290.1](https://doi.org/10.1175/JCLI-D-13-00290.1).
- Koster, R., M. J. Suarez, and M. Heiser, 2000: Variance and predictability of precipitation at seasonal-to-interannual timescales. *J. Hydrometeorol.*, **1**, 26–46, doi:[10.1175/1525-7541\(2000\)001<0026:VAPOPA>2.0.CO;2](https://doi.org/10.1175/1525-7541(2000)001<0026:VAPOPA>2.0.CO;2).
- , and Coauthors, 2004: Regions of strong coupling between soil moisture and precipitation. *Science*, **305**, 1138–1140, doi:[10.1126/science.1100217](https://doi.org/10.1126/science.1100217).
- , Y. Chang, and S. D. Schubert, 2014: A mechanism for land–atmosphere feedback involving planetary wave structures. *J. Climate*, **27**, 9290–9301, doi:[10.1175/JCLI-D-14-00315.1](https://doi.org/10.1175/JCLI-D-14-00315.1).
- Kucharski, F., N. Zeng, and E. Kalnay, 2013: A further assessment of vegetation feedback on decadal Sahel rainfall variability. *Climate Dyn.*, **40**, 1453–1466, doi:[10.1007/s00382-012-1397-x](https://doi.org/10.1007/s00382-012-1397-x).
- Lavender, S. L., C. M. Taylor, and A. J. Matthews, 2010: Coupled land–atmosphere intraseasonal variability of the West African monsoon in a GCM. *J. Climate*, **23**, 5557–5571, doi:[10.1175/2010JCLI3419.1](https://doi.org/10.1175/2010JCLI3419.1).
- Lee, E., T. N. Chase, B. Rajagopalan, R. G. Barry, T. W. Biggs, and P. J. Lawrence, 2009: Effects of irrigation and vegetation activity on early Indian summer monsoon variability. *Int. J. Climatol.*, **29**, 573–581, doi:[10.1002/joc.1721](https://doi.org/10.1002/joc.1721).
- Li, W.-P., Y. Xue, and I. Poccard, 2007: Numerical investigation of the impact of vegetation indices on the variability of West African summer monsoon. *J. Meteor. Soc. Japan*, **85A**, 363–383.
- Lohar, D., and B. Pal, 1995: The effect of irrigation on pre-monsoon season precipitation over south West Bengal, India. *J. Climate*, **8**, 2567–2570, doi:[10.1175/1520-0442\(1995\)008<2567:TEOIP>2.0.CO;2](https://doi.org/10.1175/1520-0442(1995)008<2567:TEOIP>2.0.CO;2).
- Lorenz, R., and Coauthors, 2016: Influence of land-atmosphere feedbacks on temperature and precipitation extremes in the GLACE-CMIP5 ensemble. *J. Geophys. Res. Atmos.*, **121**, 607–623, doi:[10.1002/2015JD024053](https://doi.org/10.1002/2015JD024053).
- Lu, J., and T. L. Delworth, 2005: Oceanic forcing of the late 20th century Sahel drought. *Geophys. Res. Lett.*, **32**, L22706, doi:[10.1029/2005GL023316](https://doi.org/10.1029/2005GL023316).
- May, W., A. Meier, M. Rummukainen, A. Berg, F. Cheruy, and S. Hagemann, 2015: Contributions of soil moisture interactions to

- climate change in the tropics in the GLACE–CMIP5 experiment. *Climate Dyn.*, **45**, 3275–3297, doi:10.1007/s00382-015-2538-9.
- Newell, R. E., and J. W. Kidson, 1984: African mean wind changes between Sahelian wet and dry periods. *J. Climatol.*, **4**, 27–33, doi:10.1002/joc.3370040103.
- Nicholson, S. E., and J. P. Grist, 2001: A conceptual model for understanding rainfall variability in the West African Sahel on interannual and interdecadal timescales. *Int. J. Climatol.*, **21**, 1733–1757, doi:10.1002/joc.648.
- Park, J.-Y., J. Bader, and D. Matei, 2015: Northern-Hemispheric differential warming is the key to understanding the discrepancies in the projected Sahel rainfall. *Nat. Commun.*, **6**, 5985, doi:10.1038/ncomms6985.
- Patricola, C. M., and K. H. Cook, 2007: Dynamics of the West African monsoon under mid-Holocene precessional forcing: Regional climate model simulations. *J. Climate*, **20**, 694–716, doi:10.1175/JCLI4013.1.
- , and —, 2008: Atmosphere/vegetation feedbacks: A mechanism for abrupt climate change over northern Africa. *J. Geophys. Res.*, **113**, D18102, doi:10.1029/2007JD009608.
- Rachmayani, R., M. Prange, and M. Schulz, 2015: North African vegetation–precipitation feedback in early and mid-Holocene climate simulations with CCSM3-DGVM. *Climate Past*, **11**, 175–185, doi:10.5194/cp-11-175-2015.
- Rayner, N. A., D. E. Parker, E. B. Horton, C. K. Folland, L. V. Alexander, D. P. Rowell, E. C. Kent, and A. Kaplan, 2003: Global analyses of sea surface temperature, sea ice, and night marine air temperature since the late nineteenth century. *J. Geophys. Res.*, **108**, 4407, doi:10.1029/2002JD002670.
- Reale, O., and P. Dirmeyer, 2002: Modeling the effect of land surface evaporation variability on precipitation variability. Part I: General response. *J. Hydrometeorol.*, **3**, 433–450, doi:10.1175/1525-7541(2002)003<0433:MTEOLS>2.0.CO;2.
- Roehrig, R., D. Bouniol, F. Guichard, F. Hourdin, and J. L. Redelsperger, 2013: The present and future of the West African monsoon: A process-oriented assessment of CMIP5 simulations along the AMMA transect. *J. Climate*, **26**, 6471–6505, doi:10.1175/JCLI-D-12-00505.1.
- Rowell, D. P., 2003: The impact of Mediterranean SSTs on the Sahelian rainfall season. *J. Climate*, **16**, 849–862, doi:10.1175/1520-0442(2003)016<0849:TIOMSO>2.0.CO;2.
- , C. K. Folland, K. Maskell, J. A. Owen, and M. N. Ward, 1992: Modelling the influence of global sea surface temperatures on the variability and predictability of seasonal Sahel rainfall. *Geophys. Res. Lett.*, **19**, 905–908, doi:10.1029/92GL00939.
- Schubert, S. D., M. J. Suarez, P. J. Pegion, R. D. Koster, and J. T. Bacmeister, 2004: Causes of long-term drought in the U.S. Great Plains. *J. Climate*, **17**, 485–503, doi:10.1175/1520-0442(2004)017<0485:COLDIT>2.0.CO;2.
- Seneviratne, S., T. Corti, E. Davin, M. Hirschi, E. Jaeger, I. Lehner, B. Orlowsky, and A. Teuling, 2010: Investigating soil moisture climate interactions in a changing climate: A review. *Earth-Sci. Rev.*, **99**, 125–161, doi:10.1016/j.earscirev.2010.02.004.
- , and Coauthors, 2013: Impact of soil moisture–climate feedbacks on CMIP5 projections: First results from the GLACE–CMIP5 experiment. *Geophys. Res. Lett.*, **40**, 5212–5217, doi:10.1002/grl.50956.
- Seth, A., S. A. Rauscher, M. Biasutti, A. Giannini, S. J. Camargo, and M. Rojas, 2013: CMIP5 projected changes in the annual cycle of precipitation in monsoon regions. *J. Climate*, **26**, 7328–7351, doi:10.1175/JCLI-D-12-00726.1.
- Steiner, A. L., J. S. Pal, S. A. Rauscher, J. L. Bell, N. S. Diffenbaugh, A. Boone, L. C. Sloan, and F. Giorgi, 2009: Land surface coupling in regional climate simulations of the West African monsoon. *Climate Dyn.*, **33**, 869–892, doi:10.1007/s00382-009-0543-6.
- Su, H., and J. D. Neelin, 2005: Dynamical mechanisms for African monsoon changes during the mid-Holocene. *J. Geophys. Res.*, **110**, D19105, doi:10.1029/2005JD005806.
- Sultan, B., and S. Janicot, 2000: Abrupt shift of the ITCZ over West Africa and intra-seasonal variability. *Geophys. Res. Lett.*, **27**, 3353–3356, doi:10.1029/1999GL011285.
- Taylor, C. M., 2008: Intraseasonal land–atmosphere coupling in the West African monsoon. *J. Climate*, **21**, 6636–6648, doi:10.1175/2008JCLI2475.1.
- , and R. J. Ellis, 2006: Satellite detection of soil moisture impacts on convection at the mesoscale. *Geophys. Res. Lett.*, **33**, L03404, doi:10.1029/2005GL025252.
- , A. Gounou, F. Guichard, P. P. Harris, R. J. Ellis, F. Couvreur, and M. De Kauwe, 2011: Frequency of Sahelian storm initiation enhanced over mesoscale soil-moisture patterns. *Nat. Geosci.*, **4**, 430–433, doi:10.1038/ngeo1173.
- , R. A. de Jeu, F. Guichard, P. P. Harris, and W. A. Dorigo, 2012: Afternoon rain more likely over drier soils. *Nature*, **489**, 423–426, doi:10.1038/nature11377.
- , C. E. Birch, D. J. Parker, N. Dixon, F. Guichard, G. Nikulin, and G. M. S. Lister, 2013: Modeling soil moisture–precipitation feedback in the Sahel: Importance of spatial scale versus convective parameterization. *Geophys. Res. Lett.*, **40**, 6213–6218, doi:10.1002/2013GL058511.
- Thiaw, W. M., and K. C. Mo, 2005: Impact of sea surface temperature and soil moisture on seasonal rainfall prediction over the Sahel. *J. Climate*, **18**, 5330–5343, doi:10.1175/JCLI3552.1.
- Wang, G., E. A. B. Eltahir, J. A. Foley, D. Pollard, and S. Levis, 2004: Decadal variability of rainfall in the Sahel: Results from the coupled GENESIS-IBIS atmosphere–biosphere model. *Climate Dyn.*, **22**, 625–637, doi:10.1007/s00382-004-0411-3.
- Wu, M.-L. C., O. Reale, S. D. Schubert, M. J. Suarez, R. D. Koster, and P. J. Pegion, 2009: African easterly jet: Structure and maintenance. *J. Climate*, **22**, 4459–4480, doi:10.1175/2009JCLI2584.1.
- Xue, Y., 1997: Biosphere feedback on regional climate in tropical North Africa. *Quart. J. Roy. Meteor. Soc.*, **123B**, 1483–1515, doi:10.1002/qj.49712354203.
- , and Coauthors, 2010: Intercomparison and analyses of the climatology of the West African monsoon in the West African monsoon modeling and evaluation project (WAMME) first model intercomparison experiment. *Climate Dyn.*, **35**, 3–27, doi:10.1007/s00382-010-0778-2.
- , A. Boone, and C. M. Taylor, 2012: Review of recent developments and the future prospective in West African atmosphere/land interaction. *Int. J. Geophys.*, **2012**, 748921, doi:10.1155/2012/748921.
- Zeng, N., J. D. Neelin, K. M. Lau, and C. J. Tucker, 1999: Enhancement of interdecadal climate variability in the Sahel by vegetation interaction. *Science*, **286**, 1537–1540, doi:10.1126/science.286.5444.1537.